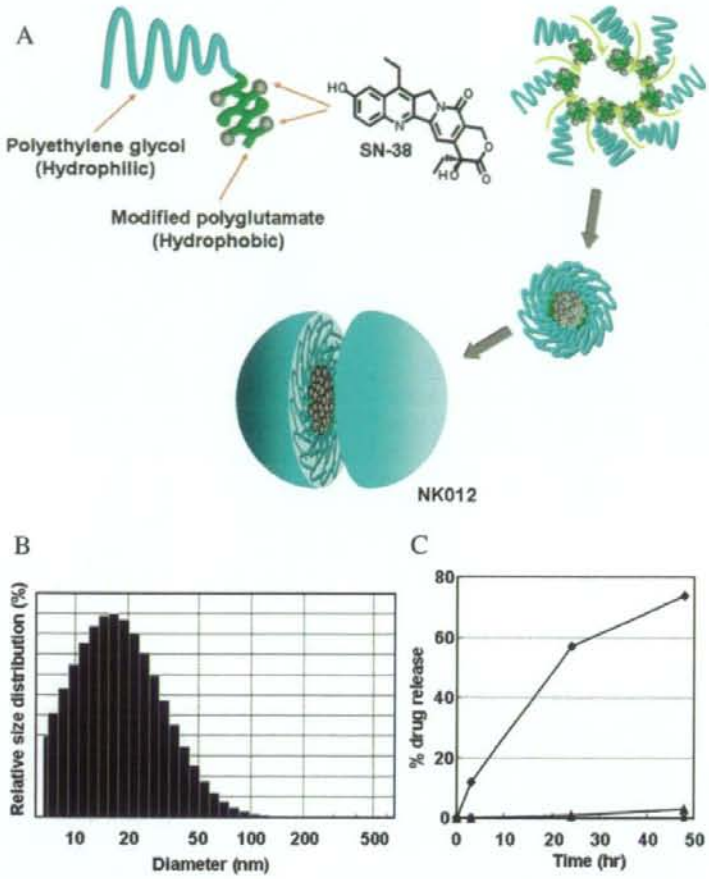

Fig. 13. Schematic structure of NK012. A polymeric micelle carrier of NK012 consists of a block copolymer of PEG (molecular weight of about 5000) and partially modified polyglutamate (about 20 unit). Polyethylene glycol (hydrophilic) is believed to be the outer shell and SN-38 was incorporated into the inner core of the micelle [56].

cytotoxic effect against each cell line as compared with CPT-11 (×43–340-fold sensitivity). On the other hand, the IC_{50} values of NK012 were a little higher than those of SN-38, similar to the cytotoxic feature also reported in a previous study about micellar drugs [39].

4.3. Pharmacokinetic analysis of NK012 and CPT-11 using HT-29-bearing nude mice

After injection of CPT-11, the concentrations of CPT-11 and SN-38 for plasma declined rapidly with time in a log–linear

Table 3
Tumor-to-plasma concentration ratio (Kp) of analytes after an intravenous administration of NK012 (30 mg/kg) to nude mice bearing human colon cancer HT-29

Test article	Analyte		Time after administration (h)						
			0.0833	1	6	24	48	72	168
NK012	P-b SN-38*	Plasma (μg/mL)	612	410	254	23.3	1.25	0.278	0.0333
		Tumor (μg/g)	4.99	8.00	13.8	9.95	5.90	5.03	3.58
		Kp (mL/g)‡	0.00815	0.0195	0.0543	0.427	4.72	18.1	108
	P-u SN-38†	Plasma (μg/mL)	3.10	1.24	0.673	0.0717	0.0127	0.00925	0.00325
		Tumor (μg/g)	0.0763	0.187	0.188	0.0904	0.0531	0.0426	0.0358
		Kp (mL/g)‡	0.0246	0.151	0.279	1.26	4.18	4.61	11.0

NOTE: Data were expressed as means of three mice [56]. * Ploymer-bound SN-38; SN-38 remaining bound to PEG-PGlu. †Polymer-unbound SN-38; free SN-38 from PEG-PGlu. ‡Kp values were calculated on the mean concentrations of three mice.

A

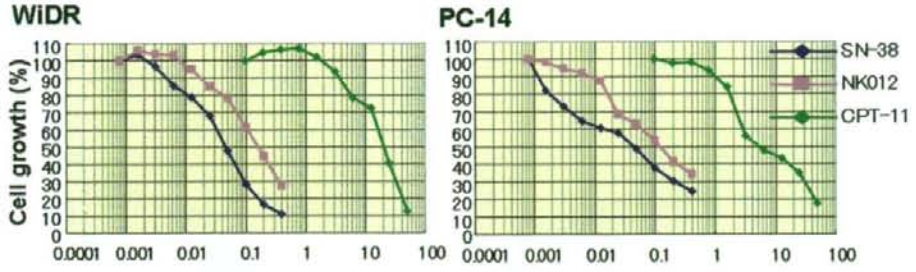

IC_{50} (μM)

cell line	SN-38	NK012	CPT-11
WiDR	0.046 ± 0.008	0.16 ± 0.014	20.4 ± 1.6
SW480	0.025 ± 0.003	0.11 ± 0.028	31.9 ± 1.3
Lovo	0.0067 ± 0.0012	0.026 ± 0.003	7.24 ± 1.04
HT-29	0.016 ± 0.003	0.068 ± 0.007	23.1 ± 2.63
PC-14	0.044 ± 0.025	0.14 ± 0.021	5.96 ± 0.90
SBC-3	0.0016 ± 0.001	0.0093 ± 0.005	0.72 ± 0.22
A431	0.0081 ± 0.002	0.019 ± 0.007	5.6 ± 1.5

B

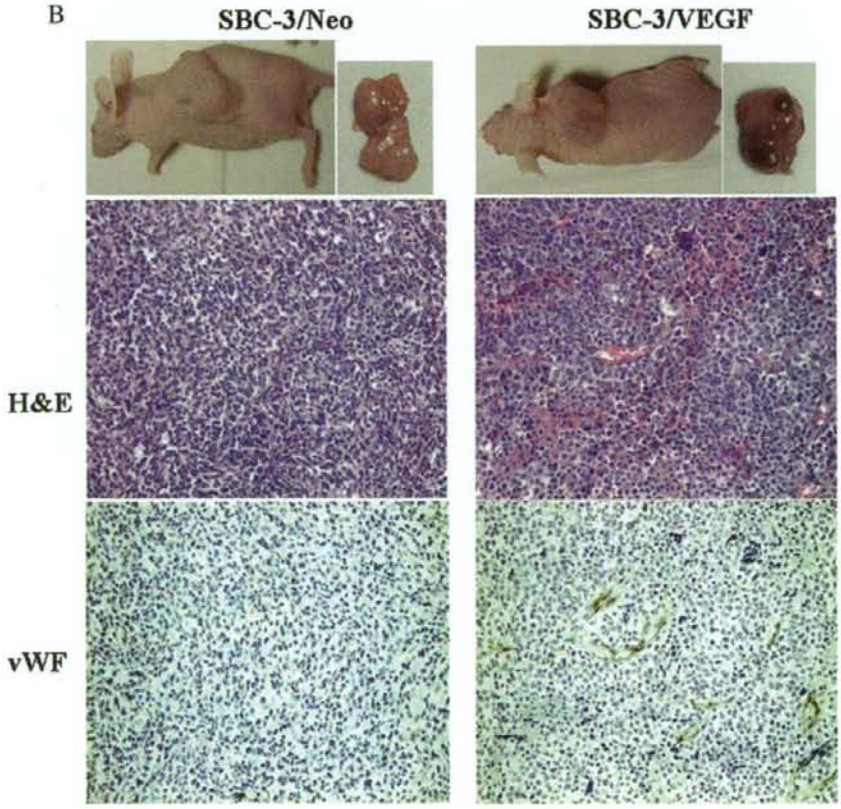

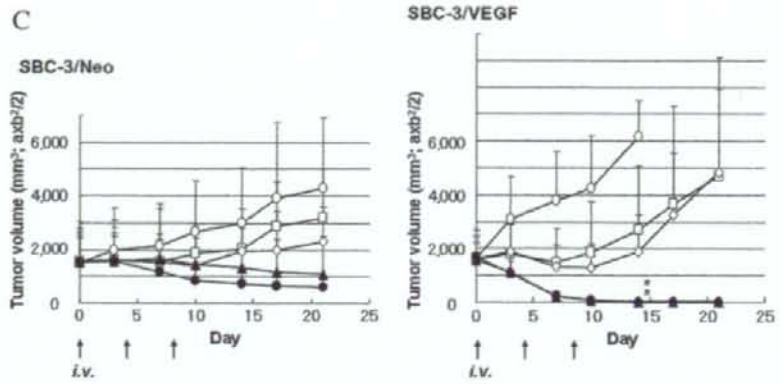

Fig. 14. Growth-inhibitory effect of NK012, SN-38, and CPT-11 on SBC-3/Neo and SBC-3/VEGF cells. (A) In *in vitro* experiment, the cells were exposed to the indicated concentrations of each drug for 72 h. The growth–inhibition curves and IC_{50} values for NK012 (▲), SN-38 (◆), and CPT-11 (■) are shown. (B) Representative photographs of massive tumors developed from SBC-3/Neo and SBC-3/VEGF at the time just before treatment initiation. Histological (H & E, ×20) and Immunohistochemical (vWF, ×20) examination for each tumor are shown. (C) Intravenous administration of NK012 or CPT-11 was started when the mean tumor volumes of groups reached a massive 1500 mm^3. The mice were divided into test group (○: control; □: CPT-11 20 mg/kg/day; ◇: CPT-11 40 mg/kg/day; ▲: NK012 15 mg/kg/day; and ●: NK012 30 mg/kg/day). NK012 or CPT-11 was administered *i.v.* on days 0, 4, and 8. Each group consisted of 4 mice. $^*P<0.05$ [56].

fashion. On the other hand, NK012 (polymer-bound SN-38) exhibited slower clearance. The clearance of NK012 in the HT-29 tumor was significantly slower and the concentration of free SN-38 was maintained at more than 30 ng/g even at 168 h after injection. The pharmacokinetic parameters of each drug in the plasma and tumor are depicted in Table 3.

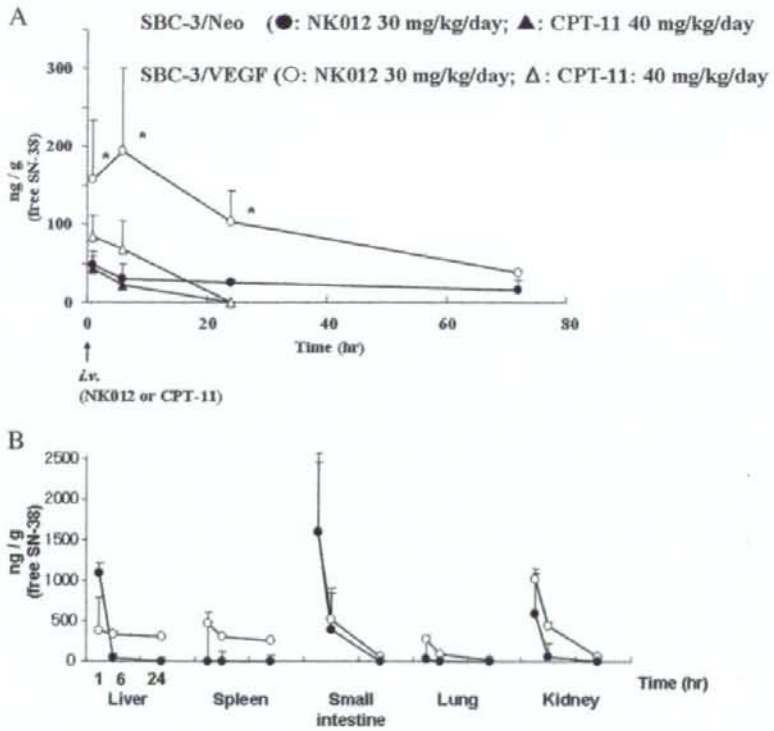

Fig. 15. Tissue and tumor distribution of free SN-38 after administration of NK012 and CPT-11. (A) Time profile of free SN-38 concentration in the SBC-3/Neo (●: NK012 30 mg/kg/day; ▲: CPT-11 40 mg/kg/day) and SBC-3/VEGF (○: NK012 30 mg/kg/day; Δ: CPT-11: 40 mg/kg/day). NK012 on day 0 and day 4 (96 h) or CPT-11 on day 0 were administered. $^*P<0.05$. (B) Tissue distribution of free SN-38 after single injection of NK012 at 30 mg/kg (○) and CPT-11 at 40 mg/kg(●) [56].

4.4. Anti-tumor activity and the distribution of NK012 and CPT-11 in SBC-3/Neo or SBC-3/VEGF tumors

In order to determine whether the potent antitumor effect of NK012 is enhanced in the tumors with high vascularity, we used vascular endothelial growth factor-secreting cells SBC-3/VEGF. There was no significant difference in the *in vitro* cytotoxic activity of each drug between SBC-3/Neo and SBC-3/VEGF (Fig. 14A). Gross findings of SBC-3/VEGF tumors are reddish as compared with SBC-3/Neo tumors (Fig. 14B). Deviating from the ordinary experimental tumor model, tumors were allowed to grow until they became massive in size, around 1.5 cm (Fig. 14C), and then the treatment was initiated. NK012 at doses of 15 and 30 mg/kg showed potent anti-tumor activity against bulky SBC-3/Neo tumors (1533.1 ± 1204.7 mm^3) as compared with CPT-11 (Fig. 14C). Striking antitumor activity was observed in mice treated with NK012 (Fig. 14C) when we compared the antitumor activity of NK012 with CPT-11 using SBC-3/VEGF cells. SBC-3/VEGF bulky masses (1620.7 ± 834.0 mm^3) disappeared in all mice, although relapse 3 months after treatment was noted in one mouse treated with NK012 20 mg/kg. On the other hand, SBC-3/VEGF were not eradicated and rapidly regrew after a partial response in mice treated with CPT-11. Approximate 10% body weight loss was observed in mice treated with NK012 20 mg/kg, but no significant difference was observed in comparison with mice treated with CPT-11 30 mg/kg.

We then examined the distribution of free SN-38 in the SBC-3/Neo and SBC-3/VEGF masses after administration of NK012 and CPT-11. In the case of CPT-11 administration, the concentrations at 1 and 6 h after the administration were less than 100 ng/g both in the SBC-3/Neo and SBC-3/VEGF tumors, and were almost negligible at 24 h in both tumors (Fig. 15A). There was no significant difference in the concentration between the SBC-3/Neo and SBC-3/VEGF tumors. On the other hand, in the case of NK012 administration, free SN-38 was detectable in the tumors even at 72 h after the administration. The concentrations of free SN-38 were higher in the SBC-3/VEGF tumors than those in the SBC-3/Neo tumors at any time point during the period of observation (significant at 1, 6, 24 h. $*P<0.05$) (Fig. 15A).

4.5. Tissue distribution of SN-38 after administration of NK012 and CPT-11

We examined the concentration-time profile of free SN-38 in various tissues after *i.v.* administration of NK012 and CPT-11. All organs measured exhibited the highest concentration of SN-38 at 1 h after administration in mice given CPT-11 (Fig. 15B). On the other hand, mice given NK012 exhibited prolonged distribution in the liver and spleen (Fig. 15B). In a similar manner to other micellar drugs [39,53], NK012 demonstrated relatively higher accumulation in organs of the reticuloendothelial system. In the lung, kidney and small intestine, the highest concentration of free SN-38 was achieved at 1 h after injection of NK012 and the concentration was almost negligible at 24 h. Although the concentrations of free SN-38 in the small intestine were relatively high at 1 h after administration of NK012 and CPT-11, those rapidly decreased. Interestingly, there was no significant difference in the kinetic character of free SN-38 in the small intestine between mice treated with NK012 and CPT-11.

4.6. Synergistic antitumor activity of the NK012 combined with 5-fluorouracil

In two phase III trials, the addition of CPT-11 to bolus or infusional 5FU/LV regimens clearly yielded greater efficacy than treatment with 5FU/LV alone, with a doubling of the tumor response rate and prolongation of the median survival time by 2–3 months [54,55].

We demonstrated that the novel SN-38-incorporating polymeric micelles, NK012, exerted superior antitumor activity and less toxicity as compared to CPT-11[53]. Therefore, we speculated that the use of NK012 in place of CPT-11 in combination with 5FU may also yield superior results.

4.6.1. Comparison of the antitumor effect of combined NK012/5FU and CPT-11/5FU

The therapeutic effect of CPT-11/5FUwas apparently inferior to that of NK012/5FU or even NK012 alone at the MTD (Fig. 13). A more potent antitumor effect, namely 100% CR rate, was obtained in the NK012 alone and NK012/5FU groups, as compared with the 0% CR rate in the CPT-11/5FU [57].

4.6.2. Specificity of cell cycle perturbation

We studied the difference in the effects between NK012 and CPT-11 on the cell cycle. The data indicate that both NK012 and CPT-11 had a tendency to accumulate the cells in the S phase, although the effect of NK012 was stronger and maintained for a more prolonged period than that of CPT-11. The histograms show aneuploidy of the tumor and that administration of NK012 or CPT-11 caused apoptosis of a proportion of the tumor cells [57].

4.7. Present situation of a clinical study of NK012

A phase 1 study of NK012 is now under way in the National Cancer Center, Tokyo and Kashiwa in patients with advanced solid tumors. NK012 is infused intravenously over 60 min every 21 days until disease progression or unacceptable toxicity occurs.

5. Conclusion

A quarter of a century has passed since the EPR effect was discovered. Now the phrase EPR has become a fundamental principle in the field of DDS. Until recently, the EPR had not been recognized in the field of oncology. However, many oncologists have now become acquainted with it, since some drugs such as doxil, abraxane, and several PEGylated proteinacious agents formulated based on the EPR have been approved in the field of oncology. Micelle carrier systems described in this chapter are obviously categorized as DDS based on the EPR. I believe that some anticancer agents incorporating micelle nanoparticles may be approved for clinical use soon.

Our next task is to develop DDS utilizing the EPR effect, which can accumulate selectively in solid tumors but also allow distribution of the delivered bullets (anticancer agents) through the entire mass of the solid tumor tissue.

References

[1] Y. Matsumura, H. Maeda, A new concept for macromolecular therapeutics in cancer chemotherapy: mechanism of tumoritropic accumulation of proteins and the antitumor agent SMANCS, Cancer Res. 46 (1986) 6387–6392.

[2] K. Kataoka, G.S. Kwon, M. Yokoyama, T. Okano, Y. Sakurai, Block copolymer micelles as vehicles for drug delivery, J. Control. Release 24 (1993) 119–132.

[3] M. Yokoyama, M. Miyauchi, N. Yamada, T. Okano, Y. Sakurai, K. Kataoka, S. Inoue, Polymer micelles as novel drug carrier: adriamycin-conjugted poly(ethylene glycol)-poly(aspartic acid) block copolymer, J. Control. Release 11 (1990) 269–278.

[4] M. Yokoyama, T. Okano, Y. Sakurai, H. Ekimoto, C. Shibazaki, K. Kataoka, Toxicity and antitumor activity against solid tumors of micelle-forming polymeric anticancer drug and its extremely long circulation in blood, Cancer Res. 51 (1991) 3229–3236.

[5] D. Khayat, E.C. Antoine, D. Coeffic, Taxol in the management of cancers of the breast and the ovary, Cancer Invest. 18 (2000) 242–260.

[6] D.N. Carney, Chemotherapy in the management of patients with inoperable non-small cell lung cancer, Semin. Oncol. 23 (1996) 71–75.

[7] R.B. Weiss, R.C. Donehower, P.H. Wiernik, T. Ohnuma, R.J. Gralla, D.L. Trump, J.R. Baker Jr, D.A. Van Echo, D.D. Von Hoff, B. Leyland-Jones, Hypersensitivity reactions from taxol, J. Clin. Oncol. 8 (1990) 1263–1268.

[8] E.K. Rowinsky, R.C. Donehower, Paclitaxel (taxol), N. Engl. J. Med. 332 (1995) 1004–1014;
R. Savic, L. Luo, A. Eisenberg, D. Maysinger, Micellar nanocontainers distribute to defined cytoplasmic organelles, Science 300 (2003) 615–618.

[9] E.K. Rowinsky, V. Chaudhry, A.A. Forastiere, S.E. Sartorius, D.S. Ettinger, L.B. Grochow, B.G. Lubejko, D.R. Cornblath, R.C. Donehower, Phase I and pharmacologic study of paclitaxel and cisplatin with granulocyte colony-stimulating factor: neuromuscular toxicity is dose-limiting, J. Clin. Oncol. 11 (1993) 2010–2020.

[10] C. Wasserheit, A. Frazein, R. Oratz, J. Sorich, A. Downey, H. Hochster, A. Chachoua, J. Wernz, A. Zeleniuch-Jacquotte, R. Blum, J. Speyer, Phase II trial of paclitaxel and cisplatin in women with advanced breast cancer: an active regimen with limiting neurotoxicity, J. Clin. Oncol. 14 (1996) 1993–1999.

[11] M. Yokoyama, T. Okano, Y. Sakurai, H. Ekimoto, C. Shibazaki, K. Kataoka, Toxicity and antitumor activity against solid tumors of micelle-forming polymeric anticancer drug and its extremely long circulation in blood, Cancer Res. 51 (1991) 3229–3236.

[12] T. Hamaguchi, Y. Matsumura, M. Susuki, K. Shimizu, R. Goda, I. Nakamura, M. Nakatomi, K. Yokoyama, K. Kataoka, T. Kakizoe, NK105, a paclitaxel-incorporating micellar nanoparticle formulation, can extend in vivo antitumour activity and reduce the neurotoxicity of paclitaxel, Br. J. Cancer 92 (2005) 1240–1246.

[13] R.B. Tishler, C.R. Geard, E.J. Hall, P.B. Schiff, Taxol sensitizes human astrocytoma cells to radiation, Cancer Res. 52 (1992) 3495–3497.

[14] H. Choy, R.F. Devore 3rd, K.R. Hande, L.L. Porter, P. Rosenblatt, F. Yunus, L. Schlabach, C. Smith, Y. Shyr, D.H. Johnson, A phase II study of paclitaxel, carboplatin, and hyperfractionated radiation therapy for locally advanced inoperable non-small-cell lung cancer (a Vanderbilt Cancer Center Affiliate Network Study), Int. J. Radiat. Oncol. Biol. Phys. 47 (2000) 931–937.

[15] M. Rodriguez, B.U. Sevin, J. Perras, H.N. Nguyen, C. Pham, A.J. Steren, O.R. Koechli, H.E. Averette, Paclitaxel: a radiation sensitizer of human cervical cancer cells, Gynecol. Oncol. 57 (1995) 165–169.

[16] B.L. Lokeshwar, S.M. Ferrell, N.L. Block, Enhancement of radiation response of prostatic carcinoma by taxol: therapeutic potential for late-stage malignancy, Anticancer Res. 15 (1995) 93–98.

[17] L. Milas, N.R. Hunter, K.A. Mason, B. Kurdoglu, L.J. Peters, Enhancement of tumor radioresponse of a murine mammary carcinoma by paclitaxel, Cancer Res. 54 (1994) 3506–3510.

[18] L. Milas, N.R. Hunter, K.A. Mason, C.G. Milross, Y. Saito, L.J. Peters, Role of reoxygenation in induction of enhancement of tumor radioresponse by paclitaxel, Cancer Res. 55 (1995) 3564–3568.

[19] A. Cividalli, G. Arcangeli, G. Cruciani, E. Livdi, E. Cordelli, D.T. Danesi, Enhancement of radiation response by paclitaxel in mice according to different treatment schedules, Int. J. Radiat. Oncol. Biol. Phys. 40 (1998) 1163–1170.

[20] R.B. Tishler, C.R. Geard, E.J. Hall, P.B. Schiff, Taxol sensitizes human astrocytoma cells to radiation, Cancer Res. 52 (1992) 3495–3497.

[21] A.G. Taghian, S.I. Assaad, A. Niemierko, I. Kuter, J. Younger, R. Schoenthaler, M. Roche, S.N. Powell, Risk of pneumonitis in breast cancer patients treated with radiation therapy and combination chemotherapy with paclitaxel, J. Natl. Cancer Inst. 93 (2001) 1806–1811.

[22] H. Choy, W. Akerley, H. Safran, S. Graziano, C. Chung, T. Williams, B. Cole, T. Kennedy, Multiinstitutional phase II trial of paclitaxel, carboplatin, and concurrent radiation therapy for locally advanced non-small-cell lung cancer, J. Clin. Oncol. 16 (1998) 3316–3322.

[23] J.E. Dowell, R. Sinard, D.A. Yardley, V. Aviles, M. Machtay, R.S. Weber, G.S. Weinstein, A.A. Chalian, D.P. Carbone, D.I. Rosenthal, Seven-week continuous-infusion paclitaxel concurrent with radiation therapy for locally advanced non-small cell lung and head and neck cancers, Semin. Radiat. Oncol. 9 (1999) 97–101.

[24] D.P. Penney, P. Rubin, Specific early fine structural changes in the lung irradiation, Int. J. Radiat. Oncol. Biol. Phys. 2 (1977) 1123–1132.

[25] P.A. Lind, L.B. Marks, P.H. Hardenbergh, R. Clough, M. Fan, D. Hollis, M.L. Hernando, D. Lucas, A. Piepgrass, L.R. Prosnitz, Technical factors associated with radiation pneumonitis after local +/− regional radiation therapy for breast cancer, Int. J. Radiat. Oncol. Biol. Phys. 52 (2002) 137–143.

[26] A.G. Taghian, S.I. Assaad, A. Niemierko, I. Kuter, J. Younger, R. Schoenthaler, M. Roche, S.N. Powell, Risk of pneumonitis in breast cancer patients treated with radiation therapy and combination chemotherapy with paclitaxel, J. Natl. Cancer. Inst. 93 (2001) 1806–1811.

[27] Y.M. Hanna, K.L. Baglan, J.S. Stromberg, F.A. Vicini, D. A Decker, Acute and subacute toxicity associated with concurrent adjuvant radiation therapy and paclitaxel in primary breast cancer therapy, Breast J. 8 (2002) 149–153.

[28] T. Negishi, F. Koizumi, H. Uchino, J. Kuroda, T. Kawaguchi, S. Naito, Y. Matsumura, NK105, a paclitaxel-incorporating micellar nanoparticle, is a more potent radiosensitising agent compared to free paclitaxel, Br. J. Cancer 95 (2006) 601–606.

[29] T. Hamaguchi, K. Kato, H. Yasui, C. Morizane, M. Ikeda, H. Uchino, K. Muro, Y. Yamada, T. Okusaka, K. Shirao, Y. Yamada, H. Nakahama, Y. Matsumura, A phase I and pharmacokinetic study of NK105, a paclitaxel-incorporating micellar nanoparticle formulation, Br. J. Cancer 97 (2007) 170–176.

[30] A. Horwich, D.T. Sleijfer, S.D. Fossa, S.B. Kaye, R.T. Oliver, M.H. Cullen, G.M. Mead, R. de Wit, P.H. de Mulder, D.P. Dearnaley, P.A. Cook, R.J. Sylvester, S.P. Stenning, Randomized trial of bleomycin, etoposide, and cisplatin compared with bleomycin, etoposide, and carboplatin in good-prognosis metastatic nonseminomatous germ cell cancer: a Multiinstitutional Medical Research Council/European Organization for Research and Treatment of Cancer Trial, J. Clin. Oncol. 15 (1997) 1844–1852.

[31] B.J. Roth, Chemotherapy for advanced bladder cancer, Semin. Oncol. 23 (1996) 633–644;
D. Screnci, M.J. McKeage, P. Galettis, T.W. Hambley, B.D. Palmer, B.C. Baguley, Relationships between hydrophobicity, reactivity, accumulation and peripheral nerve toxicity of a series of platinum drugs, Br. J. Cancer. 82 (2000) 966–972.

[32] V. Pinzani, F. Bressolle, I.J. Haug, M. Galtier, J.P. Blayac, P. Balmes, Cisplatin-induced renal toxicity and toxicity-modulating strategies: a review, Cancer Chemother. Pharmacol. 35 (1994) 1–9.

[33] M.J. Cleare, P.C. Hydes, B.W. Malerbi, D.M. Watkins, Anti-tumor platinum complexes: relationships between chemical properties and activity, Biochimie 60 (1978) 835–850.

[34] A. du Bois, H.J. Luck, W. Meier, H.P. Adams, V. Mobus, S. Costa, T. Bauknecht, B. Richter, M. Warm, W. Schroder, S. Olbricht, U. Nitz, C. Jackisch, G. Emons, U. Wagner, W. Kuhn, J. Pfisterer, A randomized clinical trial of cisplatin/paclitaxel versus carboplatin/paclitaxel as first-line treatment of ovarian cancer, J. Natl. Cancer Inst. 95 (2003) 1320–1329.

[35] J. Cassidy, J. Tabernero, C. Twelves, R. Brunet, C. Butts, T. Conroy, F. Debraud, A. Figer, J. Grossmann, N. Sawada, P. Schoffski, A. Sobrero, E. Van Cutsem, E. Diaz-Rubio, XELOX (capecitabine plus oxaliplatin): active first-line therapy for patients with metastatic colorectal cancer, J. Clin. Oncol. 22 (2004) 2084–2091.

[36] A. Horwich, D.T. Sleijfer, S.D. Fossa, S.B. Kaye, R.T. Oliver, M.H. Cullen, G.M. Mead, R. de Wit, P.H. de Mulder, D.P. Dearnaley, P.A. Cook, R.J. Sylvester, S.P. Stenning, Randomized trial of bleomycin, etoposide, and cisplatin compared with bleomycin, etoposide, and carboplatin in good-prognosis metastatic nonseminomatous germ cell cancer: a Multiinstitutional Medical Research Council/European Organization for Research and Treatment of Cancer Trial, J. Clin. Oncol. 15 (1997) 1844–1852.

[37] J. Bellmunt, A. Ribas, N. Eres, J. Albanell, C. Almanza, B. Bermejo, L.A. Sole, J. Baselga, Carboplatin-based versus cisplatin-based chemotherapy in the treatment of surgically incurable advanced bladder carcinoma, Cancer 80 (1997) 1966–1972.

[38] N. Nishiyama, S. Okazaki, H. Cabral, M. Miyamoto, Y. Kato, Y. Sugiyama, K. Nishio, Y. Matsumura, K. Kataoka, Novel cisplatin-incorporated polymeric micelles can eradicate solid tumors in mice, Cancer Res. 63 (2003) 8977–8983.

[39] H. Uchino, Y. Matsumura, T. Negishi, F. Koizumi, T. Hayashi, T. Honda, et al., Cisplatin-incorporating polymeric micelles (NC-6004) can reduce nephrotoxicity and neurotoxicity of cisplatin in rats, Br. J. Cancer 93 (2005) 678–687.

[40] L.H. Li, T.J. Fraser, E.J. Olin, B.K. Bhuyan, Action of camptothecin on mammalian cells in culture, Cancer Res. 32 (1972) 2643–2650.

[41] R.C. Gallo, J. Whang-Peng, R.H. Adamson, Studies on the antitumor activity, mechanism of action, and cell cycle effects of camptothecin, J. Natl. Cancer Inst. 46 (1971) 789–795.

[42] J.A. Gottlieb, A.M. Guarino, J.B. Call, V.T. Oliverio, J.B. Block, Preliminary pharmacologic and clinical evaluation of camptothecin sodium (NSC-100880), Cancer Chemother. Rep. 54 (1970) 461–470.

[43] F.M. Muggia, P.J. Creaven, H.H. Hansen, M.H. Cohen, O.S. Selawry, Phase I clinical trial of weekly and daily treatment with camptothecin (NSC-100880): correlation with preclinical studies, Cancer Chemother. Rep. 56 (1972) 515–521.

[44] D. Cunningham, S. Pyrhonen, R.D. James, C.J. Punt, T.F. Hickish, R. Heikkila, et al., Randomised trial of irinotecan plus supportive care versus supportive care alone after fluorouracil failure for patients with metastatic colorectal cancer, Lancet 352 (1998) 1413–1418.

[45] L.B. Saltz, J.V. Cox, C. Blanke, L.S. Rosen, L. Fehrenbacher, M.J. Moore, et al., Irinotecan plus fluorouracil and leucovorin for metastatic colorectal cancer. Irinotecan Study Group, N. Engl. J. Med. 343 (2000) 905–914.

[46] K. Noda, Y. Nishiwaki, M. Kawahara, S. Negoro, T. Sugiura, A. Yokoyama, et al., Irinotecan plus cisplatin compared with etoposide plus cisplatin for extensive small-cell lung cancer, N. Engl. J. Med. 346 (2002) 85–91.

[47] S. Negoro, N. Masuda, Y. Takada, T. Sugiura, S. Kudoh, N. Katakami, et al., CPT-11 Lung Cancer Study Group West. Randomised phase III trial of irinotecan combined with cisplatin for advanced non-small-cell lung cancer, Br. J. Cancer 88 (2003) 335–341.

[48] D.C. Bodurka, C. Levenback, J.K. Wolf, J. Gano, J.T. Wharton, J.J. Kavanagh, et al., Phase II trial of irinotecan in patients with metastatic epithelial ovarian cancer or peritoneal cancer, J. Clin. Oncol. 21 (2003) 291–297.

[49] C.H. Takimoto, S.G. Arbuck, Topoisomerase I targeting agents: the camptothecins, in: B.A. Chabner, DL Lango (Eds.), Cancer Chemotherapy and Biotherapy: Principal and Practice, 3rd ed, Lippincott Williams & Wilkins, Philadelphia (PA), 2001, pp. 579–646.

[50] J.G. Slatter, L.J. Schaaf, J.P. Sams, K.L. Feenstra, M.G. Johnson, P.A. Bombardt, et al., Pharmacokinetics, metabolism, and excretion of irinotecan (CPT-11) following I.V. infusion of [(14)C]CPT-11 in cancer patients, Drug Metab. Dispos. 28 (2000) 423–433.

[51] M.L. Rothenberg, J.G. Kuhn, H.A. Burris 3rd, J. Nelson, J.R. Eckardt, M. Tristan-Morales, et al., Phase I and pharmacokinetic trial of weekly CPT-11, J. Clin. Oncol. 11 (1993) 2194–2204.

[52] S. Guichard, C. Terret, I. Hennebelle, I. Lochon, P. Chevreau, E. Fretigny, et al., CPT-11 converting carboxylesterase and topoisomerase activities in tumor and normal colon and liver tissues, Br. J. Cancer 80 (1999) 364–370.

[53] M. Yokoyama, T. Okano, Y. Sakurai, H. Ekimoto, C. Shibazaki, K. Kataoka, Toxicity and antitumor activity against solid tumors of micelle-forming polymeric anticancer drug and its extremely long circulation in blood, Cancer Res. 51 (1991) 3229–3236.

[54] L.B. Saltz, J.Y. Douillard, N. Pirotta, et al., Irinotecan plus fluorouracil/leucovorin for metastatic colorectal cancer: a new survival standard, Oncologist 6 (2001) 81–91.

[55] J.Y. Douillard, D. Cunningham, A.D. Roth, et al., Irinotecan combined with fluorouracil compared with fluorouracil alone as first-line treatment for metastatic colorectal cancer: a multicentre randomised trial, Lancet 355 (2000) 1041–1047.

[56] F. Koizumi, M. Kitagawa, T. Negishi, et al., Novel SN-38-incorporating polymeric micelles, NK012, eradicate vascular endothelial growth factor-secreting bulky tumors, Cancer Res. 66 (2006) 10048–10056.

[57] T. Eguchi Nakajima, M. Yasunaga, Y. Kano, K. Shirao, Y. Shimada, Y. Matsumura, Synergistic antitumour activity of the novel SN-38-incorporating polymeric micelles, NK012, combined with 5-fluorouracil in a mouse model of colorectal cancer, as compared with that of irinotecan plus 5-fluorouracil, Int. J. Cancer. 122 (2008) 2148–2153.

Jpn J Clin Oncol 2008;38(12)793–802
doi:10.1093/jjco/hyn116

Review Article

Polymeric Micellar Delivery Systems in Oncology

Yasuhiro Matsumura

Investigative Treatment Division, Research Center for Innovative Oncology, National Cancer Center Hospital East, Kashiwa, Chiba, Japan

Received September 1, 2008; accepted September 22, 2008; published online November 6, 2008

The purpose of drug delivery systems in cancer chemotherapy is to achieve selective delivery of anti-cancer agents to cancer tissue at an effective concentrations for the appropriate duration of time, so that we may be able to reduce the adverse effects of a drug and simultaneously enhance the anti-tumor effect. Polymeric micelles were expected to increase the accumulation of drugs in tumor tissues utilizing the enhanced permeability and retention effect and to incorporate various kinds of drugs into the inner core by chemical conjugation or physical entrapment with relatively high stability. The size of the micelles can be controlled within the diameter range of 20–100 nm, to ensure that the micelles do not pass through normal vessel walls; therefore, a reduced incidence of the side effects of the drugs may be expected due to the decreased volume of distribution. There are several anti-cancer agent-incorporated micelle carrier systems under clinical evaluation. Phase 1 studies of a cisplatin-incorporated micelle, NC-6004 and an SN-38-incorporated micelle, NK012, are now underway. A Phase 2 study of a paclitaxel-incorporated micelle, NK105, against stomach cancer is also underway.

Key words: DDS – polymer micelles – clinical trial – EPR effect

INTRODUCTION

There are two main concepts in drug delivery system (DDS), active targeting and passive targeting. Active targeting involves monoclonal antibodies or ligands to tumor-related receptors, which can target the tumor by utilizing the specific binding ability between the antibody and antigen or between the ligand and its receptor. However, the application of DDS using monoclonal antibodies is restricted to tumors expressing high levels of related antigens. The passive targeting system can be achieved by the enhanced permeability and retention (EPR) effect (1). The EPR effect is based on the pathophysiological characteristics of solid tumor tissues: hypervascularity, incomplete vascular architecture, secretion of vascular permeability factors stimulating extravasation within cancer tissue and absence of effective lymphatic drainage from tumors, which impedes the efficient clearance of macromolecules accumulated in solid tumor tissues.

Several techniques to use maximally the EPR effect have been developed, e.g. modification of drug structures and development of drug carriers. Polymeric micelle-based anti-cancer drugs were originally developed by Prof Kataoka et al. (2–4) in the late 1980s or early 1990s. Polymeric micelles were expected to increase the accumulation of drugs in tumor tissues utilizing the EPR effect and to incorporate various kinds of drugs into the inner core by chemical conjugation or physical entrapment with relatively high stability. The size of the micelles can be controlled within the diameter range of 20–100 nm, to ensure that the micelles do not pass through normal vessel walls; therefore, a reduced incidence of the adverse effects of the drugs may be expected.

In this article, polymeric micelle systems for which clinical trials are now underway are reviewed.

For reprints and all correspondence: Yasuhiro Matsumura, Investigative Treatment Division, Research Center for Innovative Oncology, National Cancer Center Hospital East, Kashiwa, Chiba, Japan. E-mail: yhmatsum@east.ncc.go.jp

NK105, PACLITAXEL-INCORPORATING MICELLAR NANOPARTICLE

Background

Paclitaxel (PTX) is one of the most useful anti-cancer agents known for various cancers, including ovarian, breast and lung cancers (5,6). However, PTX has serious adverse effects, e.g. neutropenia and peripheral sensory neuropathy. In addition, anaphylaxis and other severe hypersensitive reactions have

been reported to develop in 2–4% of patients receiving the drug even after premedication (P) with anti-allergic agents; these adverse reactions have been attributed to the mixture of Cremophor EL and ethanol which was used to solubilize PTX (7,8). Of the adverse reactions, neutropenia can be prevented or managed effectively by administering a granulocyte colony-stimulating factor. On the other hand, there are no effective therapies to prevent or to reduce nerve damage, which is associated with peripheral neuropathy caused by PTX; therefore, neurotoxicity constitutes a significant dose-limiting toxicity (DLT) of the drug (9,10).

Preclinical Study

To construct NK105 micellar nanoparticles (Fig. 1), block copolymers consisting of polyethylene glycol and polyaspartate, the so-called PEG–polyaspartate described previously (2–4,11), were used. PTX was incorporated into polymeric micelles formed by physical entrapment utilizing hydrophobic interactions between PTX and the block copolymer polyaspartate chain (12).

Pharmacokinetic study showed that NK105 exhibited slower clearance from the plasma than PTX. The plasma concentration at 5 min (C_{5min}) and the area under the curve (AUC) of NK105 were 11- to 20-fold and 50- to 86-fold higher for NK105 than that for PTX, respectively. The maximum concentration (C_{max}) and AUC of NK105 in Colon 26 tumors were ~three times and 25 times higher for NK105 than that for PTX, respectively. NK105 continued to accumulate in the tumors until 72 h after injection (12). In *in vivo* anti-tumor activity, BALB/c mice bearing s.c. HT-29 colon cancer tumors showed decreased tumor growth rates after the administration of PTX and NK105. However, NK105 exhibited superior anti-tumor activity as compared with PTX ($P < 0.001$). The anti-tumor activity of NK105 administered at a PTX-equivalent dose of 25 mg/kg was comparable to that obtained after the administration of free PTX 100 mg/kg. Tumor suppression by NK105 increased in a dose-dependent manner. Tumors disappeared after the first dosing to mice treated with NK105 at a PTX-equivalent dose of 100 mg/kg, and all mice remained tumor-free thereafter (Fig. 2). In addition, less weight loss was induced in mice

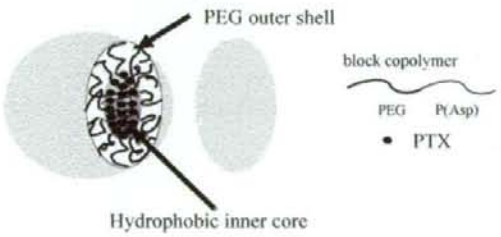

Figure 1. Preparation and characterization of NK105. The micellar structure of NK105 paclitaxel (PTX) was incorporated into the inner core of the micelle. PEG, polyethylene glycol (12).

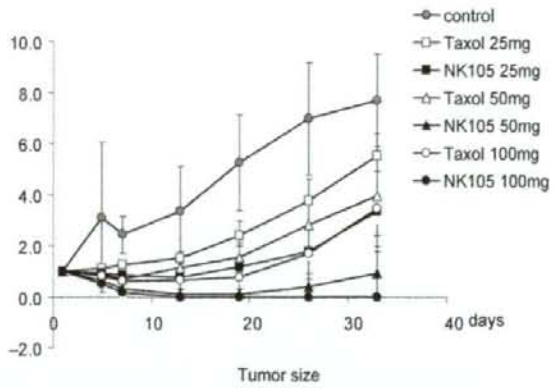

Figure 2. Effects of PTX (open symbols) and NK105 (closed symbols). PTX and NK105 were injected intravenously once weekly for 3 weeks at PTX-equivalent doses of 25 mg/kg (open square, closed square), 50 mg/kg (open triangle, closed triangle) and 100 mg/kg (open circle, closed circle), respectively. Saline was injected to control animals (open square) (12).

given NK105 100 mg/kg than in those given the same dose of free PTX (12).

Treatment with PTX has resulted in cumulative sensory-dominant peripheral neurotoxicity in humans, characterized clinically by numbness and/or paraesthesia of the extremities. Pathologically, axonal swelling, vesicular degeneration and demyelination were observed. We, therefore, examined the effects of free PTX and NK105 using both electrophysiological and morphological methods. Prior to drug administration, there were no significant differences in the amplitude of caudal sensory nerve action potential between two drug administration groups. The amplitude was significantly smaller in the PTX group than in the control group ($P < 0.01$), while the amplitude was significantly larger in the NK105 group than in the PTX group ($P < 0.05$) and was comparable between the NK105 group and the control group (Fig. 3).

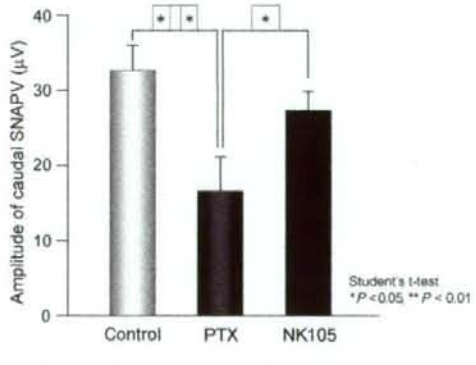

Figure 3. Effects of PTX or NK105 on the amplitude of rat caudal sensory nerve action potentials as examined 5 days after weekly injections for 6 weeks. Rats ($n = 14$) were injected with NK105 or PTX at a PTX-equivalent dose of 7.5 mg/kg. Five percent glucose was also injected in the same manner to animals in the control group (12).

Clinical Study

A Phase 1 study was designed to determine maximum tolerated dose (MTD), DLTs, the recommended dose (RD) for Phase 2 and the pharmacokinetics of NK105 (13). NK105 was administered by 1-h intravenous infusion every 3 weeks without anti-allergic P. The starting dose was 10 mg PTX-equivalent/m^2, and dose escalated according to the accelerated titration method. Nineteen patients were treated at the following doses: 10 ($n = 1$), 20 ($n = 1$), 40 ($n = 1$), 80 ($n = 1$), 110 ($n = 3$), 150 ($n = 7$) and 180 mg/m^2 ($n = 5$). Tumor types treated have included: pancreatic ($n = 11$), bile duct ($n = 5$), gastric ($n = 2$) and colon ($n = 1$). Neutropenia has been the predominant hematological toxicity and Grade 3 or 4 neutropenia was observed in patients treated at 110, 150 and 180 mg/m^2. One patient at 180 mg/m^2 developed Grade 3 fever. No other Grade 3 or 4 non-hematological toxicity including neuropathies was observed. DLTs were observed in two patients at the 180 mg/m^2 (Grade 4 neutropenia lasting for more than 5 days), which was determined as MTD. Allergic reactions were not observed in any of the patients except in one patient at 180 mg/m^2. A partial response was observed in one pancreatic cancer patient, who received more than 12 courses of NK105 (13) (Fig. 4). Despite the long-time usage, only Grade 1 or 2 neuropathy was observed by modifying the dose or period of drug administration. Colon and gastric cancer patients experienced stable disease lasting 10 and 7 courses, respectively. The C_{max} and AUC of NK105 showed dose-dependent characteristics. The plasma AUC of NK105 at 180 mg/m^2 was ~30-fold higher than that of the commonly used PTX formulation (13) (Fig. 5). DLT was Grade 4 neutropenia. NK105 generates prolonged systemic exposure to PTX in plasma. Tri-weekly 1-h infusion of NK105 was feasible and well tolerated, with anti-tumor activity in pancreatic cancer patients. A Phase 2 study of NK105 is now underway against advanced stomach cancer as a second line therapy.

NC-6004, CISPLATIN-INCORPORATING MICELLAR NANOPARTICLE

Background

Cisplatin [*cis*-dichlorodiammineplatinum (II): CDDP] is a key drug in the chemotherapy for cancers, including lung, gastrointestinal and genitourinary cancer (14,15). However, we often find that it is necessary to discontinue treatment with CDDP due to its adverse reactions, e.g. nephrotoxicity and neurotoxicity, despite its persisting effects (16). Platinum analogues, e.g. carboplatin and oxaliplatin (17), have been developed to date to overcome these CDDP-related disadvantages. Consequently, these analogues are becoming the standard drugs for ovarian (18) and colon cancers (19). However, those regimens including CDDP are considered to constitute the standard treatment for lung, stomach, testicular (20) and urothelial cancers (21). Therefore, the development of a DDS technology is anticipated, which would offer the better selective accumulation

Figure 4. Serial computed tomography (CT) scans. A 60-year-old male with pancreatic cancer, who was treated with NK105 at a dose level of 150 mg/m^2. Baseline scan (upper panels) showing multiple metastasis in the liver. Partial response, characterized by a more than 90% decrease in the size of the liver metastasis (lower panels) compared with the baseline scan. The anti-tumor response was maintained for nearly 1 year (13).

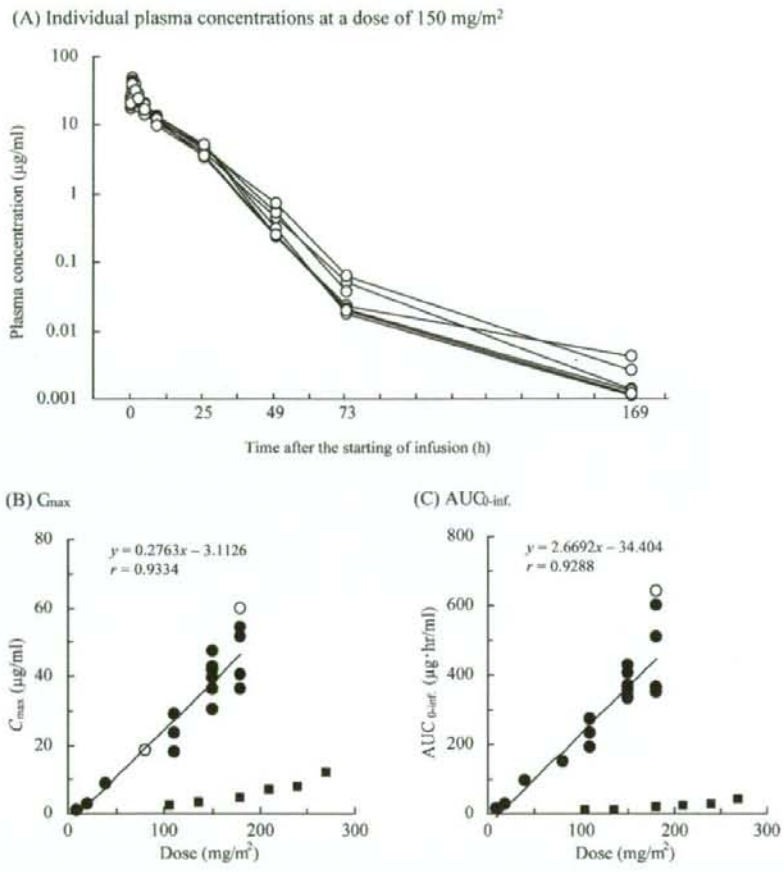

Figure 5. (A) Individual plasma concentrations of PTX in seven patients following 1 h intravenous infusion of NK105 at a dose of 150 mg/m^2. Relationships between dose and C_{max} (B), and between dose and AUC0-inf. (C) of PTX in patients following 1 h intravenous infusion of NK105. Regression analysis for dose versus C_{max} was applied using all points except for one patient at 80 mg/m^2 whose medication time became 11 min longer and one patient at 180 mg/m^2 who had medication discontinuation and steroid medication (open circle). Regression analysis for dose vs. AUC0-inf. was applied using all points except for one patient who had medication discontinuation and steroid medication (closed circle). Relationships between dose and C_{max}, and AUC0-inf in patients following conventional PTX administration were plotted (closed square) (13).

of CDDP into solid tumors while lessening its distribution into normal tissue.

Preclinical Study

NC-6004 consists of PEG, a hydrophilic chain that constitutes the outer shell of the micelles, and the coordinate complex of poly(glutamic acid) [P(Glu)] and CDDP, a polymer–metal complex-forming chain that constitutes the inner core of the micelles (22) (Fig. 6). The molecular weight of PEG-P(Glu) as a sodium salt was ~18 000 [PEG: 12 000; P(Glu): 6000]. The release rates of CDDP from NC-6004 were 19.6 and 47.8% at 24 and 96 h, respectively. In distilled water, furthermore, NC-6004 was stable without releasing cisplatin.

The AUC_{0-t} and C_{max} values were significantly higher in animals given NC-6004 than in animals given CDDP, namely, 65- and 8-fold, respectively ($P < 0.001$ and 0.001, respectively) (23). The C_{max} in tumor was 2.5-fold higher for NC-6004 than for CDDP ($P < 0.001$). Furthermore, the tumor AUC was 3.6-fold higher for NC-6004 than for CDDP (81.2 and 22.6 μg/ml h in animals given NC-6004 and CDDP, respectively) (23).

BALB/c nude mice implanted with a human gastric cancer cell line MKN-45 showed decreased tumor growth rates after i.v. injection of CDDP and NC-6004 (Fig. 7A). The NC-6004 administration groups at the same dose levels as CDDP showed no significant difference in tumor growth rate. Regarding time-course changes in body weight change rate, the CDDP 5 mg/kg administration group showed a significant decrease ($P < 0.001$) in body weight as compared with the control group. On the other hand, NC-6004 administration group did not show a decrease in body weight as compared with the control group (Fig. 7B).

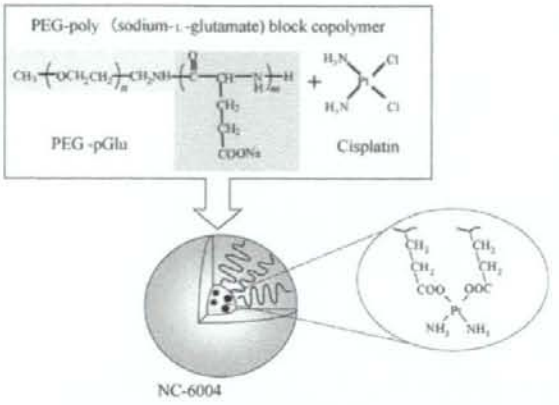

Figure 6. Preparation and characterization of cisplatin (CDDP)-incorporating polymeric micelles (NC-6004). Chemical structures of CDDP and polyethylene glycol poly(glutamic acid) block copolymers [PEG-P(Glu) block copolymers], and the micellar structures of CDDP-incorporating polymeric micelles (NC-6004) (22).

Regarding toxicity, the CDDP 10 mg/kg administration group showed significantly higher plasma concentrations of blood urea nitrogen and creatinine as compared with the control group ($P < 0.05$ and 0.001, respectively), with the NC-6004 10 mg/kg administration group ($P < 0.05$ and 0.001, respectively) (Fig. 8A and B). Light microscopy indicated tubular dilation with flattening of the lining cells of the tubular epithelium in the kidney from all animals in the CDDP 10 mg/kg administration group. On the other hand, no histopathologic change was observed in the kidneys from all animals in the NC-6004 10 mg/kg administration group (data not shown). Animals given NC-6004 showed no delay in sensory nerve condition velocities (SNCVs) as compared with animals given 5% glucose. On the other hand, animals given CDDP showed a significant delay ($P < 0.05$) in SNCV as compared with animals given NC-6004 (Fig. 9A). The analysis by ICP-MS on sciatic nerve concentrations of platinum showed that the concentrations were significantly ($P < 0.05$) lower in animals given NC-6004 (Fig. 9B). This finding is believed to be a factor that reduced neurotoxicity following NC-6004 administration as compared with the CDDP administration (23).

Clinical Study

A Phase 1 trial was run in two UK experimental cancer medicine centers with the PK assays performed in a good laboratory practice-accredited laboratory in Newcastle University (24).

Patients with solid tumors were included in this open-label trial. Usual Phase 1 inclusion and exclusion criteria were applied, including adequate renal function. Patients were limited to one previous course of platinum-based treatment with maximum dose limits of cisplatin, carboplatin or oxaliplatin.

Dose escalation proceeded in two stages. In Stage 1, we recruited cohorts of one to three patients until Grade 2 toxicity was seen in Cycle 1. In Stage 2, we had cohorts of three patients expanding to six if one of three DLT and to confirm MTD.

The starting dose for the Phase 1 study was 10 mg/m^2. NC-6004 was administered as a 60 min infusion with a total infusion volume of 500 ml. Treatment was repeated on a 3-weekly cycle until progressive disease, intolerance of the agent or patient withdrawal. Pharmacokinetic analysis of total plasma platinum (Pt), micellar Pt and ultrafiltrate Pt (UF Pt) was performed using WinNonlin version 1.3 to calculate C_{max}, T_{max}, half-life and AUC for all Pt species. Clearance and volume of distribution were calculated based on the measurements of total and micellar Pt.

In this trial, 17 patients (10 male, 7 female) were treated. The median age (range) was 59 years (40–80), and tumor

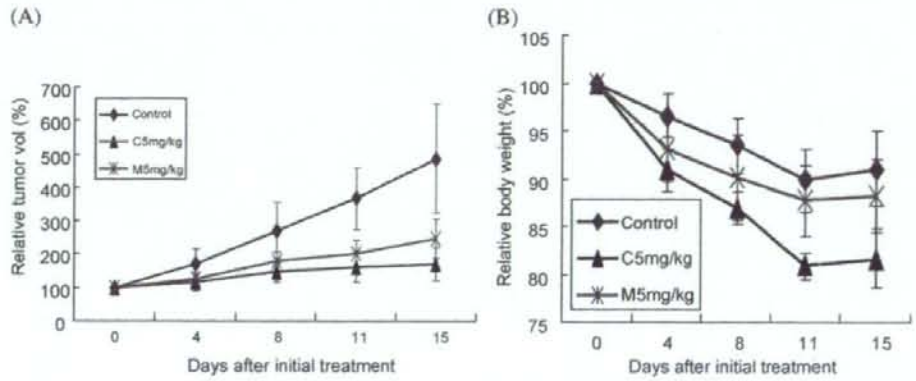

Figure 7. Relative changes in MKN-45 tumor growth rates in nude mice. (A) CDDP (closed triangle) and NC-6004 (cross symbol) were injected intravenously every 3 days, three administrations in total, at CDDP-equivalent doses of 5 mg/kg. Five percent glucose was injected in the control mice (open diamond). (B) Changes in relative body weight. Data were derived from the same mice as those used in the present study. Values are expressed as the mean ± SE (23).

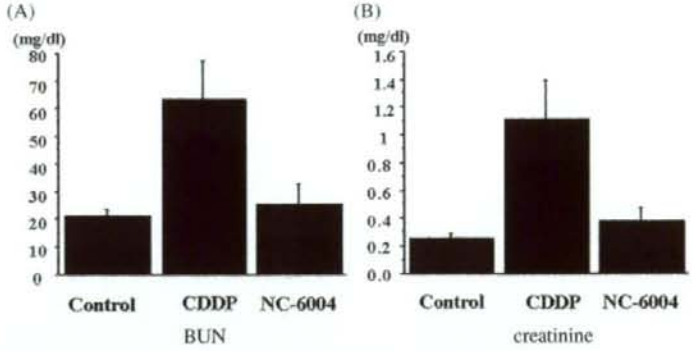

Figure 8. Nephrotoxicity of CDDP and NC-6004. Plasma concentrations of blood urea nitrogen (BUN) and creatinine were measured after a single i.v. injection of 5% glucose ($n = 8$), CDDP at a dose of 10 mg/kg ($n = 12$), NC-6004 at a dose of 10 mg/kg ($n = 13$) on a CDDP basis (23).

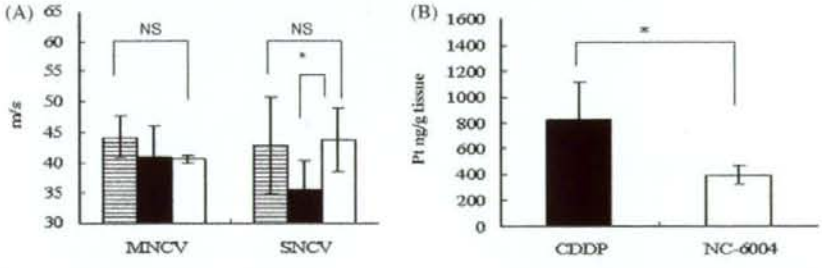

Figure 9. Neurotoxicity of CDDP and NC-6004 in rats. Rats ($n = 5$) were given CDDP (2 mg/kg), NC-6004 (an equivalent dose of 2 mg/kg CDDP), or 5% glucose, all intravenously twice a week, 11 administrations in total. Sensory nerve conduction velocity and motor nerve conduction velocity of the sciatic nerve at Week 6 after the initial administration (A). The platinum concentration in the sciatic nerve. Rats were given CDDP (5 mg/kg, $n = 5$), NC-6004 (an equivalent dose of 5 mg/kg CDDP, $n = 5$) or 5% glucose ($n = 2$), all intravenously twice a week, four administrations in total. On Day 3 after the final administration, a segment of the sciatic nerve was removed and the platinum concentration in the sciatic nerve was measured by ICP-MS (B). The data are expressed as the mean ± SD. $^*P < 0.05$ (23).

types included colorectal (4), NSCLC (3), esophageal (2), pancreatic (2), melanoma (2) and one each of GIST, mesothelioma, renal cell and hepatocellular cancer. Treatment was well tolerated with little nausea (no routine use of prophylactic antiemetics) and no protocol-defined DLTs were observed. There was no myelotoxicity or neurotoxicity and no changes in audiometry (Table 1).

A Grade 2 fall in ethylenediamine tetraacetic acid (EDTA) glomerular filtration rate (GFR) was observed at 40 mg/m^2, and post-hydration (H) with 1L N saline IV over 30 min for all patients was therefore instituted and followed by administration of doses up to 120 mg/m^2 without significant nephrotoxicity. Four hypersensitivity reactions occurred in the first nine patients on or after Cycle 2. After introduction of P with anti-histamines and corticosteroids, two further reactions were seen, during the third or fourth cycle. Three patients had previous platinum exposure, and three were platinum-naïve (Table 1).

The best response was stable disease and this was seen in seven of 17 (41%) patients.

In the ultrafiltrate fraction, there was delayed (T_{max} = 24 h) and prolonged (half-life 68–580 h) detection of small molecular weight platinum species. NC-6004 provides a sustained release of potentially active platinum species. Using gel-filtration, we have been able to separate the Pt present in the original formulation from other Pt species in the plasma. The kinetics of UF Pt indicated a delayed and sustained release of cisplatin after dosing with NC-6004.

This novel formulation of cisplatin is well tolerated with minimal nephrotoxicity and no significant myelosuppression, emesis or neurotoxicity but a higher rate of hypersensitivity reactions than predicted. Disease stabilization has been seen in heavily pre-treated patients with efficacy best assessed in future Phase 2 trials. The recommended Phase 2 dose of NC-6004 for monotherapy is 90–120 mg/m^2 and for the combination is 60–90 mg/m^2.

NK012, SN-38-INCORPORATING MICELLAR NANOPARTICLE

Background

The anti-tumor plant alkaloid camptothecin (CPT) is a broad-spectrum anti-cancer agent that targets the DNA

Table 1. Patient results of NC-6004 Phase 1 trial

Dose level (mg/m^2)	No of patients	No of cycles (median)	Renal impairment	EDTA GFR change (ml/min)	Hypersensitivity (cycle)	Best response
1 (10)	1	3			Gr 2 (C3)	SD
2 (20)	1	2				PD
3 (40)	3	1–4 (2)	Gr 2 (C1)	95 → 39		1 SD
						2 PD
4 (60)	3	2 (2)			Gr 1 (C2)	1 NE
+ H					Gr 3 (C2)	2 PD
5 (90)	6	2–4 (2)	Gr 2 (C1)	74 → 59	Gr 3 (C4)	3 SD
+H			Gr 2 (C2)	67 → 53		3 PD
6 (120)	3	2–4 (3)			Gr 2 (C4)	2 SD
+ H + P					Gr 3 (C3)	1 PD

A Grade 2 fall in EDTA GFR was observed at 40 mg/m^2 and hydration with 1000 ml saline i.v. over 30 mm for all patients was therefore instituted and following this administration of doses up to 120 mg/m^2 without significant nephrotoxicity was performed (24). EDTA, ethylenediamine tetraacetic acid; GFR, glomerular filtration rate; Gr, grade; C, cycle; SD, standard deviationl; PD, progressive disease; NE, not evaluated.

topoisomerase I. Although CPT has showed promising anti-tumor activity *in vitro* and *in vivo* (25,26), it has not been used clinically because of its low therapeutic efficacy and severe toxicity (27,28). Among CPT analogs, irinotecan hydrochloride (CPT-11) has recently been demonstrated to be active against colorectal, lung and ovarian cancers (29–33). CPT-11 itself is a prodrug and is converted to 7-ethyl-10-hydroxy-CPT (SN-38), a biologically active metabolite of CPT-11, by carboxylesterases (CEs). SN-38 exhibits up to 1000-fold more potent cytotoxic activity against various cancer cells *in vitro* than CPT-11 (34). Although CPT-11 is converted to SN-38 in the liver and tumor, the metabolic conversion rate is $<10\%$ of the original volume of CPT-11 (35,36). In addition, the conversion of CPT-11 to SN-38 depends on the genetic inter-individual variability of CE activity (37). Thus, the direct use of SN-38 might be of great advantage, and attractive, for cancer treatment. For the clinical use of SN-38, however, it is essential to develop a soluble form of water-insoluble SN-38. The progress of the manufacturing technology of 'micellar nanoparticles' may make it possible to utilize SN-38 for *in vivo* experiments and further clinical use.

Preclinical Study

SN-38 was bound to the carboxylic acid on a polyglutamate (PGlu) chain of block copolymer through the ester bond. NK012 is an SN-38-loaded polymeric micelle constructed in an aqueous milieu by the self-assembly of an amphiphilic block copolymer, PEG–PGlu(SN-38) (38) (Fig. 10). The mean particle size of NK012 is 20 nm in diameter with a relatively narrow range. The releasing rates of SN-38 from NK012 in phosphate-buffered saline at 37°C were 57 and 74% at 24 and 48 h, respectively, and that in 5% glucose solution at 37°C were 1 and 3% at 24 and 48 h, respectively. These results indicate that NK012 can release SN-38 under neutral conditions even without the presence of a hydrolytic enzyme and is stable in 5% glucose solution. It is suggested that NK012 is stable before administration and starts to release SN-38, the active component, under physiological conditions after administration.

In PK study, after injection of CPT-11, the concentrations of CPT-11 and SN-38 for plasma declined rapidly with time in a log-linear fashion. On the other hand, NK012 (polymer-bound SN-38) exhibited slower clearance. The clearance of NK012 in the HT-29 tumor was significantly slower and the concentration of free SN-38 was maintained at >30 ng/g even at 168 h after injection. Anti-tumor activity of NK012 was evaluated in lung (38), renal (39), pancreatic (40) and stomach cancers xenografts (41) in comparison with CPT-11. NK012 exhibited superior anti-tumor activity in all tumors tested compared with CPT-11. Also, the therapeutic effect of NK012/5FU was significantly superior to that of CPT-11/5FU against the HT-29 xenografts ($P = 0.0004$). A 100% CR rate was obtained in the NK012/5FU group, as compared with the 0% CR rate in the CPT-11/5FU (Fig. 11) (42).

It may be concluded that NK012 can selectively accumulate in any tumor xenografts, to be distributed effectively throughout the entire body of the tumor, including in hypovascular tumors, and show sustained-release for a prolonged period of time. Consequently, NK012 can exert more significant anti-tumor activity as compared with CPT-11, which is not an ideal formulation for realizing the time-dependent actions of the drug (40).

Clinical Study

Two independent Phase 1 studies of NK012 have been almost completed in the National Cancer Center in Japan (43) and the Sarah Canon Cancer Center in the USA (44) in patients with advanced solid tumors to determine the

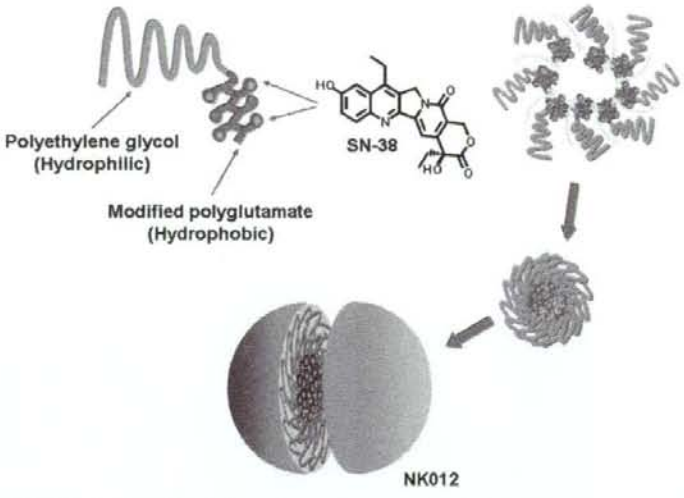

Figure 10. Schematic structure of NK012. A polymeric micelle carrier of NK012 consists of a block copolymer of PEG (molecular weight of ~5000) and partially modified polyglutamate (~20 U). Polyethylene glycol (hydrophilic) is believed to be the outer shell and SN-38 was incorporated into the inner core of the micelle (38).

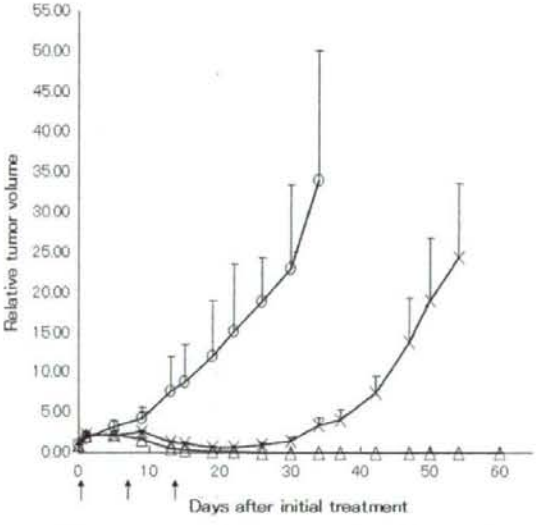

Figure 11. Effect of NK012/5-FU as compared with that of CPT-11/5-FU against HT-29 tumor-bearing mice. (Open circle) control, (cross symbol) CPT-11 50 mg/kg 24 h before 5-FU 50 mg/kg, (closed triangle) NK012 10 mg/kg 24 h before 5-FU 50 mg/kg (42).

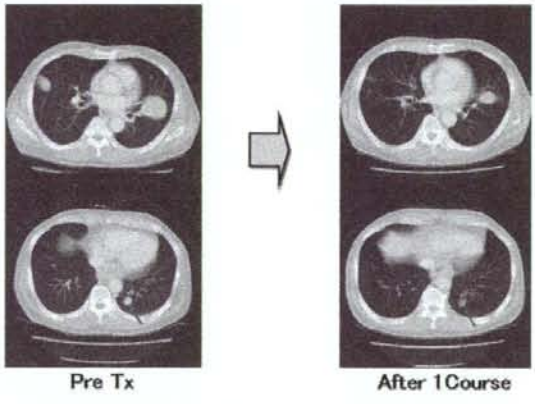

Figure 12. CT scan of an esophageal cancer patient with lung metastasis. This patient had previously undergone 5-FU+CDDP followed by taxotere. Partial response, characterized by a more than 50% decrease in size of the lung metastasis compared with the baseline scan (43).

pharmacokinetics, toxicity profile and the RD for Phase 2 of NK012. NK012 is infused intravenously over 30 min every 21 days until disease progression or unacceptable toxicity occurs. UGT1A1 genotype screening was performed prior to enrollment, and UGT1A1*28/*28 homozygotes were treated at a reduced dose level with the potential for dose escalation based on toxicities. In a Japanese study, the starting dose was 2 mg/m^2 as an SN-38 equivalent, and the dose was escalated by the accelerated titration method. In an US study, the starting dose was 9 mg/m^2 as an SN-38 equivalent and at least three patients were treated at each dose level.

DLT was determined to be neutropenia. MTD will become >28 mg/m^2 and RD may become ≤28 mg/m^2. Non-hematological toxicities including diarrhea were mostly less than Grade 2 in Course 1. One partial response has been reported in a patient with esophageal cancer in a Japanese study (Fig. 12), and three patients with triple negative breast cancer and one patient with small cell lung cancer had PR in the US study. In conclusion, NK012 is well tolerated and has demonstrated anti-tumor activity in patients with refractory tumors.

CONCLUSION

A quarter of a century has passed since the EPR effect was discovered. Until recently, the EPR had not been recognized in the field of oncology. However, many oncologists have now become acquainted with it, since some drugs such as doxil, abraxane and several PEGylated proteinacious agents formulated based on the EPR have been approved in the field of oncology. Micelle carrier systems described in this article are obviously categorized as DDS based on the EPR. It is expected that some anti-cancer agents incorporating micelle nanoparticles may be approved for clinical use soon.

Our next task is to develop DDS, which can accumulate selectively in solid tumors but also allow distribution of the delivered bullets (anti-cancer agents) through the entire mass of the solid tumor tissue.

Funding

This work was supported partly by a Grant-in-Aid from the 3rd Term Comprehensive Control Research for Cancer, Ministry of Health, Labor and Welfare (Y. Matsumura) and Scientific Research on Priority Areas from the Ministry of Education, Culture, Sports, Science and Technology (Y. Matsumura), and the Princess Takamatsu Cancer Research Fund (Y. Matsumura).

Conflict of interest statement

None declared.

References

1. Matsumura Y, Maeda H. A new concept for macromolecular therapeutics in cancer chemotherapy: mechanism of tumoritropic accumulation of proteins and the antitumor agent smancs. *Cancer Res* 1986;46:6387–92.
2. Kataoka K, Kwon GS, Yokoyama M, Okano T, Sakurai Y. Block copolymer micelles as vehicles for drug delivery. *J Controlled Release* 1993;24:119–32.
3. Yokoyama M, Miyauchi M, Yamada N, Okano T, Sakurai Y, Kataoka K, et al. Polymer micelles as novel drug carrier: adriamycin-conjugated poly(ethylene glycol)-poly(aspartic acid) block copolymer. *J Controlled Release* 1990;11:269–78.
4. Yokoyama M, Okano T, Sakurai Y, Ekimoto H, Shibazaki C, Kataoka K. Toxicity and antitumor activity against solid tumors of micelle-forming polymeric anticancer drug and its extremely long circulation in blood. *Cancer Res* 1991;51:3229–36.
5. Khayat D, Antoine EC, Coeffic D. Taxol in the management of cancers of the breast and the ovary. *Cancer Invest* 2000;18:242–60.
6. Carney DN. Chemotherapy in the management of patients with inoperable non-small cell lung cancer. *Semin Oncol* 1996;23:71–5.
7. Weiss RB, Donehower RC, Wiernik PH, Ohnuma T, Gralla RJ, Trump DL, et al. Hypersensitivity reactions from taxol. *J Clin Oncol* 1990;8:1263–8.
8. Rowinsky EK, Donehower RC. Paclitaxel (taxol). *N Engl J Med* 1995;332:1004–14.
9. Rowinsky EK, Chaudhry V, Forastiere AA, Sartorius SE, Ettinger DS, Grochow LB, et al. Phase I and pharmacologic study of paclitaxel and cisplatin with granulocyte colony-stimulating factor: neuromuscular toxicity is dose-limiting. *J Clin Oncol* 1993;11:2010–20.
10. Wasserheit C, Frazein A, Oratz R, Sorich J, Downey A, Hochster H, et al. Phase II trial of paclitaxel and cisplatin in women with advanced breast cancer: an active regimen with limiting neurotoxicity. *J Clin Oncol* 1996;14:1993–9.
11. Yokoyama M, Okano T, Sakurai Y, Ekimoto H, Shibazaki C, Kataoka K. Toxicity and antitumor activity against solid tumors of micelle-forming polymeric anticancer drug and its extremely long circulation in blood. *Cancer Res* 1991;51:3229–36.
12. Hamaguchi T, Matsumura Y, Suzuki M, Shimizu K, Goda R, Nakamura I, et al. NK105, a paclitaxel-incorporating micellar nanoparticle formulation, can extend in vivo antitumour activity and reduce the neurotoxicity of paclitaxel. *Brit J Cancer* 2005;92:1240–6.
13. Hamaguchi T, Kato K, Yasui H, Morizane C, Ikeda M, Ueno H, et al. A Phase I and Pharmacokinetic Study of NK105, a paclitaxel-incorporating micellar nanoparticle formulation. *Brit J Cancer* 2007;97:170–6.
14. Horwich A, Sleijfer DT, Fossa SD, Kaye SB, Oliver RT, Cullen MH, et al. Randomized trial of bleomycin, etoposide, and cisplatin compared with bleomycin, etoposide, and carboplatin in good-prognosis metastatic nonseminomatous germ cell cancer: a Multiinstitutional Medical Research Council/European Organization for Research and Treatment of Cancer Trial. *J Clin Oncol* 1997;15:1844–52.
15. Roth BJ. Chemotherapy for advanced bladder cancer. *Semin Oncol* 1996;23:633–44.
16. Pinzani V, Bressolle F, Haug IJ, Galtier M, Blayac JP, Balmes P. Cisplatin-induced renal toxicity and toxicity-modulating strategies: a review. *Cancer Chemother Pharmacol* 1994;35:1–9.
17. Cleare MJ, Hydes PC, Malerbi BW, Watkins DM. Anti-tumor platinum complexes: relationships between chemical properties and activity. *Biochimie* 1978;60:835–50.
18. du Bois A, Luck HJ, Meier W, Adams HP, Mobus V, Costa S, et al. A randomized clinical trial of cisplatin/paclitaxel versus carboplatin/paclitaxel as first-line treatment of ovarian cancer. *J Natl Cancer Inst* 2003;95:1320–9.
19. Cassidy J, Tabernero J, Twelves C, Brunet R, Butts C, Conroy T, et al. XELOX (capecitabine plus oxaliplatin): active first-line therapy for patients with metastatic colorectal cancer. *J Clin Oncol* 2004;22:2084–91.
20. Horwich A, Sleijfer DT, Fossa SD, Kaye SB, Oliver RT, Cullen MH, et al. Randomized trial of bleomycin, etoposide, and cisplatin compared with bleomycin, etoposide, and carboplatin in good-prognosis metastatic nonseminomatous germ cell cancer: a Multiinstitutional Medical Research Council/European Organization for Research and Treatment of Cancer Trial. *J Clin Oncol* 1997;15:1844–52.
21. Bellmunt J, Ribas A, Eres N, Albanell J, Almanza C, Bermejo B, et al. Carboplatin-based versus cisplatin-based chemotherapy in the treatment of surgically incurable advanced bladder carcinoma. *Cancer* 1997;80:1966–72.
22. Nishiyama N, Okazaki S, Cabral H, Miyamoto M, Kato Y, Sugiyama Y, et al. Novel cisplatin-incorporated polymeric micelles can eradicate solid tumors in mice. *Cancer Res* 2003;63:8977–83.
23. Uchino H, Matsumura Y, Negishi T, Hayashi T, Honda T, Nishiyama N, et al. Cisplatin-incorporating polymeric micelles (NC-6004) can reduce nephrotoxicity and neurotoxicity of cisplatin in rats. *Brit J Cancer* 2005;93:678–87.
24. Wilson RH, Plummer R, Adam J, Eatock MM, Boddy AV, Griffin M, et al. Phase I and pharmacokinetic study of NC-6004, a new platinum entity of cisplatin-conjugated polymer forming micelles. *Am Soc Clin Oncol* 2008; (Abs# 2573).
25. Li LH, Fraser TJ, Olin EJ, Bhuyan BK. Action of camptothecin on mammalian cells in culture. *Cancer Res* 1972;32:2643–50.
26. Gallo RC, Whang-Peng J, Adamson RH. Studies on the antitumor activity, mechanism of action, and cell cycle effects of camptothecin. *J Natl Cancer Inst* 1971;46:789–95.
27. Gottlieb JA, Guarino AM, Call JB, Oliverio VT, Block JB. Preliminary pharmacologic and clinical evaluation of camptothecin sodium (NSC-100880). *Cancer Chemother Rep* 1970;54:461–70.
28. Muggia FM, Creaven PJ, Hansen HH, Cohen MH, Selawry OS. Phase I clinical trial of weekly and daily treatment with camptothecin (NSC-100880): correlation with preclinical studies. *Cancer Chemother Rep* 1972;56:515–21.
29. Cunningham D, Pyrhonen S, James RD, Punt CJ, Hickish TF, Heikkila R, et al. Randomised trial of irinotecan plus supportive care versus supportive

care alone after fluorouracil failure for patients with metastatic colorectal cancer. *Lancet* 1998;352:1413–8.
30. Saltz LB, Cox JV, Blanke C, Rosen LS, Fehrenbacher L, Moore MJ, et al. Irinotecan plus fluorouracil and leucovorin for metastatic colorectal cancer. Irinotecan Study Group. *N Engl J Med* 2000;343: 905–14.
31. Noda K, Nishiwaki Y, Kawahara M, Negoro S, Sugiura T, Yokoyama A, et al. Irinotecan plus cisplatin compared with etoposide plus cisplatin for extensive small-cell lung cancer. *N Engl J Med* 2002;346:85–91.
32. Negoro S, Masuda N, Takada Y, Sugiura T, Kudoh S, Katakami N, et al., CPT-11 Lung Cancer Study Group West. Randomised phase III trial of irinotecan combined with cisplatin for advanced non-small-cell lung cancer. *Br J Cancer* 2003;88:335–41.
33. Bodurka DC, Levenback C, Wolf JK, Gano J, Wharton JT, Kavanagh JJ, et al. Phase II trial of irinotecan in patients with metastatic epithelial ovarian cancer or peritoneal cancer. *J Clin Oncol* 2003;21:291–7.
34. Takimoto CH, Arbuck SG. Topoisomerase I targeting agents: the camptothecins. In: Chabner BA, Lango DL editors. Cancer Chemotherapy and Biotherapy: Principal and Practice, 3rd edn. Philadelphia (PA): Lippincott Williams & Wilkins 2001;579–646.
35. Slatter JG, Schaaf LJ, Sams JP, Feenstra KL, Johnson MG, Bombardt PA, et al. Pharmacokinetics, metabolism, and excretion of irinotecan (CPT-11) following I.V. infusion of [(14)C]CPT-11 in cancer patients. *Drug Metab Dispos* 2000;28: 423–33.
36. Rothenberg ML, Kuhn JG, Burris HA, 3rd, Nelson J, Eckardt JR, Tristan-Morales M, et al. Phase I and pharmacokinetic trial of weekly CPT-11. *J Clin Oncol* 1993;11:2194–204.
37. Guichard S, Terret C, Hennebelle I, Lochon I, Chevreau P, Fretigny E, et al. CPT-11 converting carboxylesterase and topoisomerase activities in tumor and normal colon and liver tissues. *Br J Cancer* 1999;80: 364–70.
38. Koizumi F, Kitagawa M, Negishi T, et al. Novel SN-38-incorporating polymeric micelles, NK012, eradicate vascular endothelial growth factor-secreting bulky tumors. *Cancer Res* 2006;66:10048–56.
39. Sumitomo M, Koizumi F, Asano T, Horiguchi A, Ito K, Asano T, et al. Novel SN-38-incorparated polymeric micelles, NK012, strongly suppress renal cancer progression. *Cancer Res* 2008;122:2148–53.
40. Saito Y, Yasunaga M, Kuroda J, Koga Y, Matsumura Y. Enhanced distribution of NK012 and prolonged sustained-release of SN-38 within tumors are the key strategic point for a hypovascular tumor. *Cancer Sci* 2008;99:1258–64.
41. Nakajima-Eguchi T, Yanagihara K, Takigahara M, Yasunaga M, Kato K, Hamaguchi T, et al. Antitumor effect of SN-38-releasing polymeric micelles, NK012, on spontaneous peritoneal metastases from orthotopic gastoric cancer in mice compared with irinotecan. *Cancer Res* 2008 (in press).
42. Nakajima T, Yasunaga M, kano Y, Koizumi F, Kato K, Hamaguchi T, et al. Synergistic antitumor activity of the novel SN-38 incorporating polymeric micelles, NK012, combined with 5-fluorouracil in a mouse model of colorectal cancer, as compared with that of irinotecan plus 5-fluorouracil. *Int J Cancer* 2008;122:22148–53.
43. Kato K, Hamaguchi T, Shirao K, Shimada Y, Yamada Y, Doi T, et al. Phase I study of NK012, polymer micelle SN-38, in patients with advanced cancer. *Am Soc Clin Oncol GI* 2008; (Abs#485).
44. Burris HA, III, Infante JR, Spigel DR, Greco FA, Thompson DS, Matsumoto S, et al. A phase I dose-escalation study of NK012. *Am Soc Clin Oncol* 2008; (Abs#2538).

Research Article

Antitumor Effect of SN-38–Releasing Polymeric Micelles, NK012, on Spontaneous Peritoneal Metastases from Orthotopic Gastric Cancer in Mice Compared with Irinotecan

Takako Eguchi Nakajima,[1,2] Kazuyoshi Yanagihara,[3] Misato Takigahira,[3] Masahiro Yasunaga,[1] Ken Kato,[2] Tetsuya Hamaguchi,[2] Yasuhide Yamada,[2] Yasuhiro Shimada,[2] Keichiro Mihara,[5] Takahiro Ochiya,[4] and Yasuhiro Matsumura[1]

[1]Investigative Treatment Division, Research Center for Innovative Oncology, National Cancer Center Hospital East, Kashiwa, Chiba, Japan; [2]Gastrointestinal Oncology Division, National Cancer Center Hospital, [3]Central Animal Laboratory, and [4]Section for Studies on Metastasis, National Cancer Center Research Institute, Tokyo, Japan; and [5]Hematology and Oncology Department, Clinical and Experimental Oncology Division, Research Institute for Radiation Biology and Medicine, Hiroshima University, Hiroshima, Japan

Abstract

7-Ethyl-10-hydroxy-camptothecin (SN-38), an active metabolite of irinotecan hydrochloride (CPT-11), has potent antitumor activity. Moreover, we have reported the strong antitumor activity of NK012 (i.e., SN-38–releasing polymeric micelles) against human cancer xenografts compared with CPT-11. Here, we investigated the advantages of NK012 over CPT-11 treatment in mouse models of gastric cancer with peritoneal dissemination. NK012 or CPT-11 was i.v. administered thrice every 4 days at their respective maximum tolerable doses (NK012, 30 mg/kg/day; CPT-11, 67 mg/kg/day) to mice receiving orthotopic transplants of gastric cancer cell lines (44As3Luc and 58As1mLuc) transfected with the luciferase gene (n = 5). Antitumor effect was evaluated using the photon counting technique. SN-38 concentration in gastric tumors and peritoneal nodules was examined by high-performance liquid chromatography (HPLC) 1, 24, and 72 hours after each drug injection. NK012 or CPT-11 distribution in these tumors was evaluated using a fluorescence microscope on the same schedule. In both models, the antitumor activity of NK012 was superior to that of CPT-11. High concentrations of SN-38 released from NK012 were detected in gastric tumors and peritoneal nodules up to 72 hours by HPLC. Only a slight conversion from CPT-11 to SN-38 was observed from 1 to 24 hours. Fluorescence originating from NK012 was detected up to 72 hours, whereas that from CPT-11 disappeared until 24 hours. NK012 also showed antitumor activity against peritoneal nodules. Thus, NK012 showing enhanced distribution with prolonged SN-38 release may be ideal for cancer treatment because the antitumor activity of SN-38 is time dependent. [Cancer Res 2008;68(22):9318–22]

Introduction

Gastric cancer is the second most common cause of death from cancer in the world. The survival rate has remained low in patients with advanced gastric cancer, with a median survival rate of 13 months having been recently reported in a phase III trial, which has been the best outcome thus far (1). Patients with gastric cancer with scirrhous type stroma particularly showed poor prognosis even after curative resection, as well as highly progressed peritoneal dissemination (2). Because peritoneal dissemination causes several refractory symptoms such as massive ascites, intestinal obstruction, hydronephrosis, and obstructive jaundice, the quality of life of patients at the end stage of cancer is severely impaired.

Poor delivery of anticancer drugs to peritoneal metastatic cells may be one of the reasons for the poor prognosis of patients with peritoneal dissemination (3). In peritoneal nodules, the distribution and eventual diffusion of drugs to cancer cells tend to be impeded because of several obstacles such as severe fibrosis and high interstitial pressure (4, 5). On the other hand, angiogenesis was reported to be an essential factor in the development of peritoneal metastasis, and the high expression level of vascular endothelial growth factor (VEGF) in primary gastric tumors or ascitic fluid, which can enhance tumor vascular permeability, was found to be directly associated with the development of ascites and peritoneal dissemination (6–10). In addition, several factors such as kinins and nitric oxide are involved in tumor vascular permeability (11–13). Polymer-conjugated drugs and nanoparticles categorized under drug delivery system agents are favorably extravasated from the vessels into the interstitium of tumors due to the enhanced permeability and retention effect (EPR effect; refs. 14, 15). The EPR effect is based on the following pathophysiologic characteristics of solid tumor tissues: hypervascularity, incomplete vascular architecture, secretion of vascular permeability factors stimulating extravasation within cancer tissue, and absence of effective lymphatic drainage from the tumors that impedes the efficient clearance of macromolecules accumulated in solid tumor tissues. Moreover, macromolecules cannot freely leak out from normal vessels, and thus, the side effects of an anticancer agent can be reduced. Very recently, we have shown that NK012 (i.e., SN-38–releasing polymeric micelles) exerted superior antitumor activity and less toxicity than CPT-11 (15–17). In a series of studies, we showed that NK012 markedly enhanced the antitumor activity of SN-38, particularly against highly VEGF-secreting SBC-3/VEGF tumors compared with SBC-3/Neo tumors. On the other hand, it is conceivable that satisfactory drug delivery cannot be achieved in less-vascularized and highly fibrotic tumors, particularly for macromolecules. However, we observed that NK012 showed a strong antitumor activity even in the xenograft of Capan1 cells, which are pancreatic cancer cells with abundant stromal tissue, compared with CPT-11. This result suggests that NK012 can selectively accumulate in both hypervascular and hypovascular tumors with high interstitial pressure, and then induce sustained

Requests for reprints: Yasuhiro Matsumura, Investigative Treatment Division, Research Center for Innovative Oncology, National Cancer Center Hospital East, 6-5-1 Kashiwanoha, Kashiwa, Chiba 277-8577, Japan. Phone: 81-4-7134-6857; Fax: 81-4-7134-6866; E-mail: yhmatsum@east.ncc.go.jp.

doi:10.1158/0008-5472.CAN-08-2822

release of SN-38, followed by SN-38 distribution throughout the entire tumor tissues. In the present study, we evaluated the antitumor activity of NK012 against peritoneal tumor dissemination compared with that of CPT-11 using mouse models orthotopically transplanted with scirrhous gastric cancer cells, as well as against spontaneously progressing peritoneal dissemination (18, 19).

Materials and Methods

Cell cultures. 44As3 and 58As1m were previously reported as human signet-ring cell gastric cancer cell lines that spontaneously metastasize to the peritoneal cavity and produce large volumes of bloody ascites after orthotopic implantion in the gastric wall (18–21). Here, 44As3 and 58As1m cells were transfected with a complex of 4 μg of pEGF-PLuc plasmid DNA (Clontech) and 24 μL of GeneJammer reagent (Stratagene; Cloning Systems) in accordance with the manufacturer's instructions. Stable transfectants were selected in geneticin (400 μg/mL; Invitrogen), and bioluminescence was used to screen transfected clones for luciferase gene expression using the IVIS system (Xenogen). Clones expressing the luciferase gene were named 44As3Luc and 58As1mLuc. 44As3Luc and 58As1mLuc cells were maintained in RPMI 1640 supplemented with 10% FCS (Sigma), 100 IU/mL penicillin G sodium, and 100 mg/mL streptomycin sulfate (Immuno-Biological Laboratories) in a humidified atmosphere containing 5% CO_2 at 37°C.

Orthotopic models *in vivo*. Six-week-old female BALB/c *nu/nu* mice were purchased from CLEA Japan, Inc., and maintained under specific pathogen-free conditions and provided with sterile food, water, and cages. Ambient light was controlled to provide regular cycles of 12 h of light and 12 h of darkness. A total of 1×10^6 cells of 44As3Luc or 58As1Luc were inoculated into the gastric wall of each mouse after laparotomy, as described previously (18–21). *In vivo* photon counting analysis was conducted on a cryogenically cooled IVIS system using Living Image acquisition and analysis software (Xenogen). All animal procedures were performed in compliance with the Guidelines for the Care and Use of Experimental Animals established by the Committee for Animal Experimentation of the National Cancer Center; these guidelines conform to the ethical standards required by law and also comply with the guidelines for the use of experimental animals in Japan.

Drugs. NK012 was prepared by Nippon Kayaku Co., Ltd. (15). CPT-11 was purchased from Yakult Honsha Co., Ltd.

***In vivo* growth inhibition assay.** After inoculation of 44As3Luc or 58As1mLuc cells into the gastric wall (day 0), mice were randomly divided into test groups consisting of 5 mice per group. 44As3Luc mice were i.v. administered the maximum tolerated dose (MTD) of the 2 drugs via the tail vein on days 20, 24, and 28 as previously reported, that is, at 66.7 mg/kg/d for CPT-11 and 30 mg/kg/d for NK012 (15). 58As1mLuc mice were given the drugs in the same manner on days 18, 22, and 26. Photon counting analysis and body weight were measured twice a week. "Visible ascites," which was evident a few days before death in this mouse model, was used as a surrogate for survival time in consideration of animal welfare. Mice were euthanized when ascites became visible, and colonization of gastric wall by cancer cells and metastasis to the peritoneal cavity were confirmed in all the euthanized mice. Differences in relative photon counts between the treatment groups at day 42 in 44As3Luc mice and at day 81 in 58As1mLuc mice were analyzed using the unpaired *t* test.

Assay of free SN-38 in tissues. We next analyzed the biodistributions of NK012 and CPT-11 to orthotopic gastric tumors and peritoneal nodules. Twenty-six days after the inoculation of 44As3Luc cells into the gastric wall of mice, NK012 (30 mg/kg) or CPT-11 (66.7 mg/kg) was administered via the tail vein. Under anesthesia, orthotopic gastric tumor and peritoneal nodule samples were excised 1, 24, and 72 hours after injection.

Measurements of tissue concentration of free SN-38 by high-performance liquid chromatography. Samples were rinsed with physiologic saline, mixed with 0.1 mol/L glycine-HCl buffer (pH 3.0)/methanol at 5 w/w%, and then homogenized. To analyze the concentration of free SN-38, 100 μL of the tumor samples were mixed with 20 μL of 1 mmol/L phosphoric acid/methanol (1:1) and 40 μL of ultrapure water, and camptothecin (CPT) was used as the internal standard (10 ng/mL for free SN-38). The samples were vortexed vigorously for 10 s, and then filtered

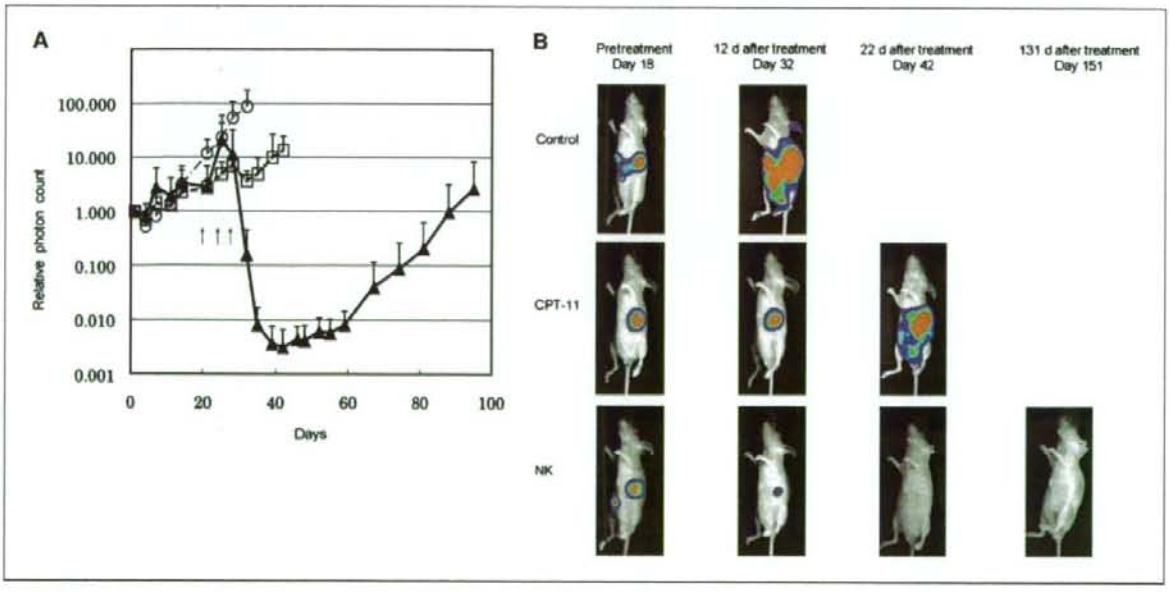

Figure 1. Effects of NK012 and CPT-11 in 44As3Luc mouse models. *A*, antitumor activity of NK012 or CPT-11 was evaluated by counting the number of photons using the IVIS system (*points*, mean; *bars*, SD; *arrows*, drug injections). Antitumor effect of each regimen on days 20, 24, and 28. (○), control; (□), CPT-11 (66.7 mg/kg/d, ×3); and (▲), NK012 (30 mg/kg/d, ×3) in 44As3Luc mouse model. *B*, images of 44As3Luc mouse model administered NK012 taken using the IVIS system on days 18, 32, 42, and 151 after inoculation of 44As3Luc cells. Data were derived from the same mice as those used in the present study.

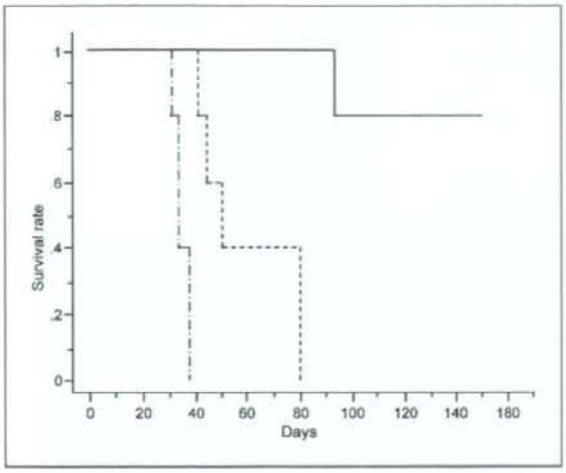

Figure 2. Survival curves of 44As3Luc mouse models. Survival curves of 44As3Luc mouse model in each regimen on days 20, 24, and 28. (–·–·–), control; (- - -), CPT-11 given at 66.7 mg/kg/d ×3; and (——), NK012 given at 30 mg/kg/d ×3.

through Ultrafree-MC Centrifugal Filter Devices with a cutoff molecular diameter of 0.45 μm (Millipore Co.). Reversed-phase high-performance liquid chromatography (HPLC) was conducted at 35°C on a Mightysil RP-18 GP column (150 × 4.6 mm; Kanto Chemical Co., Inc.). Fifty microliters of a sample were injected into an Alliance Water 2795 HPLC system (Waters) equipped with a Waters 2475 multi λ fluorescence detector. Fluorescence originating from SN-38 was detected at 540 nm with an excitation wavelength of 365 nm. The mobile phase was a mixture of 100 mmol/l ammonium acetate (pH 4.2) and methanol [11:9 (v/v)], and the flow rate was 1.0 mL/min. The content of SN-38 was calculated by measuring the relevant peak area and calibrating against the corresponding peak area derived from the CPT internal standard. Peak data were recorded using a chromatography management system (MassLynx v4.0; Waters).

Visualization of distribution of NK012 and CPT-11 by fluorescence microscopy. Mice were given fluorescein *Lycopersicon esculentum* lectin (100 μL per mouse; Vector Laboratories) to visualize tumor vasculature in the samples 5 min before anesthesia. The samples were then excised and embedded in an optimal cutting temperature compound (Sakura Finetechnochemical Co., Ltd.) and frozen at −80°C. Six-μm-thick tumor sections were then prepared using a cryostatic microtome, Tissue-Tek Cryo3 (Sakura Finetechnochemical Co., Ltd.). Frozen sections were examined under a fluorescence microscope, BIOZERO (KEYENCE), at an excitation wavelength of 377 nm and an emission wavelength 447 nm to evaluate the distribution of NK012 and CPT-11. Both drugs could be detected under the same fluorescence conditions because formulations containing SN-38 bound via ester bonds possess a particular fluorescence.

Statistical analyses. Data were expressed as mean ± SD. Data were analyzed using the Student's *t* test when groups showed equal variances (*F* test), or the Welch's test when they showed unequal variances (*F* test). *P* value of <0.05 was considered as significant. All statistical tests were two sided.

Results

Antitumor activities of NK012 and CPT-11. Comparison of the relative photon counts on day 42 in the 44As3Luc mouse model revealed significant differences in counts between mice given with NK012 and those given with CPT-11 ($P = 0.0282$; Fig. 1*A* and *B*). Similar result was obtained in the experiment with 58As gastric tumor (data not shown). The survival rates on day 150 in the 44As3Luc mouse model were 80% and 0% for the NK012 group and CPT-11 group, respectively (Fig. 2). Similar result was obtained in the experiment with 58As gastric tumor (data not shown). No marked toxic effects in terms of body weight changes were observed in any groups for any mouse models (data not shown). Only 1 mouse in the CPT-11 group of 44As1 mouse models showed diarrhea for 3 d, and any other clinical symptoms were not observed.

Tissue concentrations of free SN-38 after administration of NK012 and CPT-11. We examined the concentration-time profile of free SN-38 in orthotopic gastric tumors and peritoneal nodules in the 44As3Luc mouse model after the administration of NK012 and CPT-11 (Fig. 3*A* and *B*). Either orthotopic gastric tumors or peritoneal nodules exhibited the highest concentration of free SN-38 24 hours after NK012 administration, and 1 hour after CPT-11 administration. The highest concentrations of free SN-38 in the NK012 group were much higher than those in the CPT-11 group in either orthotopic gastric tumors or peritoneal nodules. The concentrations of free SN-38 released from NK012 in orthotopic gastric tumors were higher than those in peritoneal nodules.

Tumor tissue distribution of NK012 and CPT-11 as determined by fluorescence microscopy. Results showed that NK012 accumulation in either orthotopic gastric tumors or peritoneal nodules had been maintained from 1 hour to 72 hours after injection (Fig. 4*A*). On the other hand, CPT-11 showed maximum accumulation in either orthotopic gastric tumors or peritoneal nodules 1 hour after injection and disappeared within 24 hours (Fig. 4*B*).

Discussion

The main purpose of this study was to clarify the advantages of NK012 over CPT-11 as treatment against peritoneal metastasis spontaneously disseminated from orthotopically transplanted scirrhous gastric cancer cells in mouse models. We showed that NK012 exerted more potent antitumor activity in the mouse models used than CPT-11. Therefore, NK012 is considered promising in terms of providing clinical benefit to patients with gastric cancer showing progressing peritoneal dissemination.

CPT-11 is converted to SN-38, a biologically active and water-insoluble metabolite of CPT-11, by carboxylesterases (CE) in the liver and tumors. However, only 2% to 8% of administered CPT-11 is converted by CE in the liver and tumors to the active form SN-38 (22, 23). The conversion of CPT-11 to SN-38 also depends on genetic interindividual variability of the activity of CE (24). Thus, the direct use of SN-38 might be of great advantage and is attractive for cancer treatment. We have recently shown that NK012 (i.e., SN-38–releasing polymeric micelles) exerted superior antitumor activity and less toxicity than CPT-11 (15–17). The mean particle size of NK012 is 20 nm in diameter. NK012 can release SN-38 under neutral conditions even in the absence of CE because SN-38, which is bound to the blockcopolymer by phenolic ester binding, is stable under acidic conditions but relatively labile under neutral and mild alkaline conditions. The release rate of SN-38 from NK012 under physiologic conditions is quite high, that is, >70% of SN-38 is gradually released within 48 hours.

In this study, we used mouse models with orthotopically transplanted human scirrhous gastric cancer cells showing spontaneously progressing peritoneal dissemination, which we

reported previously (18, 19, 21). These models can imitate more realistically the progressing mode of human peritoneal dissemination of gastric cancer than conventional experimental models directly transplanted with cancer cells i.p. Moreover, our models enabled us to quantitatively evaluate drug antitumor effect even against peritoneal dissemination without having to sacrifice the animal and perform autopsy through the use of gastric cancer cells transfected with the luciferase gene and by applying photon counting analysis, having already verified the significant correlation between tumor volume and photon counts in a previous report (19).

For *in vivo* growth inhibition assay, drug administration was started on day 18 or 20 after cell inoculation into the gastric wall, when small peritoneal metastatic nodules and a small degree of ascites had appeared. The present results showed that NK012 had more potent antitumor activity than CPT-11 in the mouse models tested, suggesting its effectiveness against peritoneal dissemination of gastric cancer in the clinical setting.

In the pharmacologic evaluation, we could confirm the more enhanced distribution of NK012 than CPT-11 to not only orthotopic gastric tumors but also peritoneal nodules by quantifying SN-38 concentration in the tumors and visualization of fluorescence originating from NK012 or CPT-11 distributed in the tumors. Because CPT-11 or SN-38 has been reported to possess time-dependent growth-inhibitory activity against tumor cells, this prolonged retention of NK012 in the tumors and the sustained release of free SN-38 from NK012 may be responsible for its more potent antitumor activity observed in the present study (25). On the other hand, CPT-11 disappeared from the tumors before exerting sufficient antitumor activity. For both drugs, however, the concentrations of SN-38 in orthotopic gastric tumors were higher than those

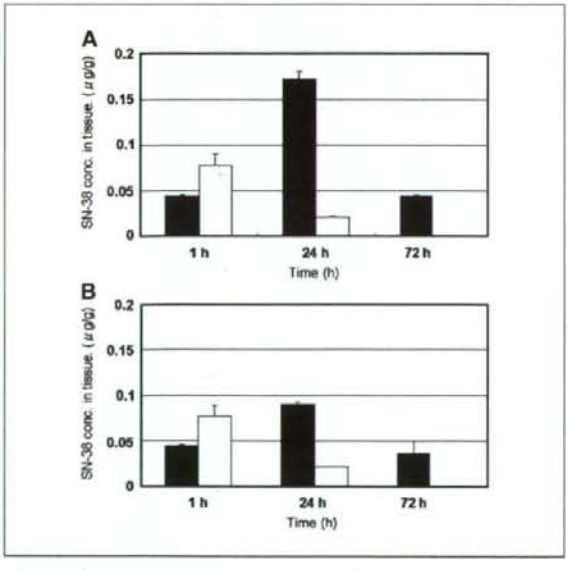

Figure 3. Concentration-time profile of free SN-38. NK012 (30 mg/kg) or CPT-11 (66.7 mg/kg) was injected 26 d after implantation of 44As3Luc gastric cancer cells (*columns*, mean; *bars*, SD). *A*, concentration (*conc.*) of free SN-38 in orthotopic gastric tumor tissue of 44As3Luc mouse model after administration of NK012 (*black column*) and CPT-11 (*white column*). *B*, concentration of free SN-38 in peritoneal nodules of 44As3Luc mouse model after administration of NK012 (*black column*) and CPT-11 (*white column*).

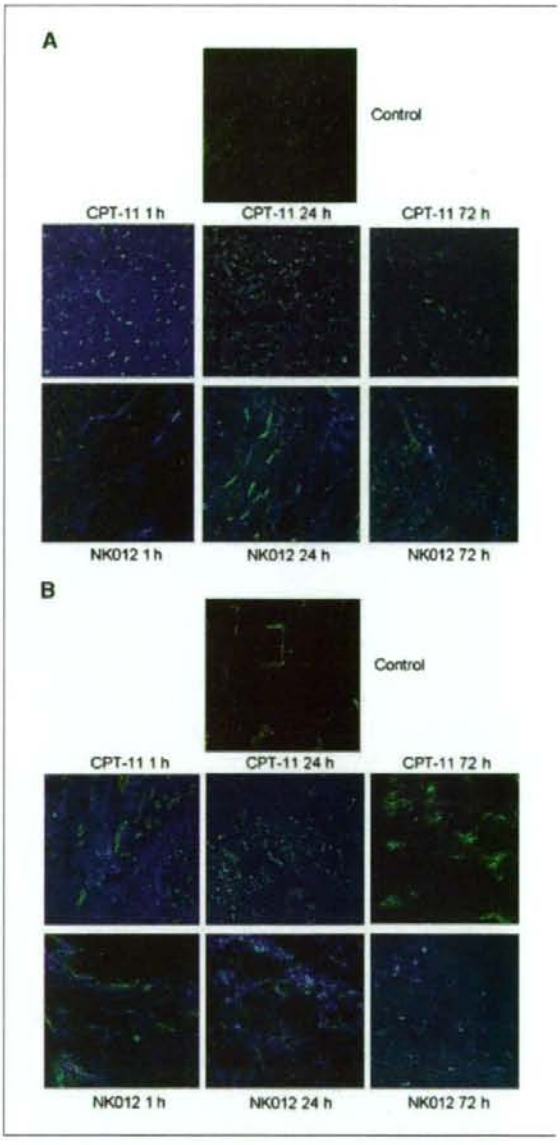

Figure 4. Tissue distribution of NK012 and CPT-11 as determined by fluorescence microscopy. Orthotopic gastric tumors or peritoneal nodules of 44As3Luc mouse model were excised 1, 24, and 72 h after i.v. injection of NK012 (30 mg/kg) or CPT-11 (66.7 mg/kg). Each mouse was i.v. administered with fluorescein-labeled *Lycopersicon esculentum* lectin just before being sacrificed to detect tumor blood vessels. Frozen sections were examined under a fluorescence microscope at an excitation wavelength of 377 nm and an emission wavelength of 447 nm. The same fluorescence condition can be applied for visualizing NK012 and CPT-11 fluorescence. Free SN-38 cannot be detected under this fluorescence condition. *A*, distribution of NK012 or CPT-11 in orthotopic gastric tumors (×100). *B*, distribution of NK012 or CPT-11 in peritoneal nodules (×100).

in peritoneal nodules. This is consistent with previous reports stating the poor delivery of anticancer drugs to peritoneal metastatic cells probably because of some obstacles such as abundant interstitium or high interstitial pressure. To date, we reported that NK012 can